Quaternary Science Reviews 77 (2013) 210–227

Contents lists available at SciVerse ScienceDirect

Quaternary Science Reviews

journal homepage: www.elsevier.com/locate/quascirev

Formation of mega-scale glacial lineations on the Dubawnt Lake Ice Stream bed: 2. Sedimentology and stratigraphy

C. Ó Cofaigh [a,*], C.R. Stokes [a], O.B. Lian [b], C.D. Clark [c], S. Tulaczyk [d]

[a] Department of Geography, Durham University, Durham DH1 3LE, UK
[b] Department of Geography, University of the Fraser Valley, Abbotsford, B.C., Canada
[c] Department of Geography, University of Sheffield, UK
[d] Department of Earth and Planetary Sciences, University of California, Santa Cruz, CA, USA

ARTICLE INFO

Article history:
Received 23 January 2013
Received in revised form
26 June 2013
Accepted 27 June 2013
Available online 30 August 2013

Keywords:
Mega-scale glacial lineations
Ice streams
Dubawnt Lake Palaeo-Ice Stream
Sedimentology
Subglacial bedforms

ABSTRACT

Mega-scale glacial lineations (MSGLs) are highly elongate, subglacial landforms produced beneath zones of fast-flowing ice. While qualitative data on their morphology have existed for several decades, studies of their composition and sedimentology are comparatively rare. Sediment exposures along the course of the Finnie River in Nunavut, northern Canada, provide a window into the internal stratigraphy and sedimentology of MSGLs formed by the Dubawnt Lake Palaeo-Ice Stream during regional deglaciation of the Laurentide Ice Sheet. Stratigraphic sections record evidence for an initial advance of ice into the study area followed by ice sheet recession and deposition of glacifluvial and glacilacustrine outwash. Subsequently, the Dubawnt Lake Palaeo-Ice Stream overrode and reworked this outwash subglacially forming an 'MSGL till'. This till comprises a sandy, red diamicton facies, forming the core of the MSGL ridges and containing variably deformed lenses, stringers and rafts of outwash. The sedimentology of this diamicton is consistent with an origin as a glacitectonite and hybrid till formed by a combination of non-pervasive subglacial sediment deformation and lodgement. Facies variations from stratified to massive diamicton reflect, in turn, variations in strain and subglacial transport distance. The occurrence of stratified glacifluvial sediments within these ridges and the well-preserved nature of many of the sandy inclusions within the diamicton imply relatively short transport distances and incomplete mixing. MSGLs under the Dubawnt Lake Palaeo-Ice Stream formed through a combination of subglacial erosion and deposition. This included non-pervasive, subglacial sediment deformation and the reworking of pre-existing sediment depocentres during streaming flow. These results highlight the importance of sediment supply to MSGL formation with the presence of abundant pre-existing sediments which were subsequently overridden being critical to lineation formation.

1. Introduction

Mega-scale glacial lineations (MSGLs) are highly elongate, subglacial landforms formed in sediment and with lengths typically greater than 10 km. They were formally recognized and defined by Clark (1993) on the basis of mapping from satellite imagery, and they have since been recorded in both modern and palaeo-, marine and terrestrial, glacial settings (e.g., Kleman and Borgström, 1996; Shipp et al., 1999; Clark and Stokes, 2001; Ó Cofaigh et al., 2002, 2010a; Stokes and Clark, 2002; Ottesen et al., 2005; Heroy and Anderson, 2005; King et al., 2009). MSGLs are formed in association with ice streams, which are corridors of ice flowing at speeds of 100 s−1000 s of metres per year and moving much faster than the ice on either side. Formation of MSGLs occurs at the ice stream bed and, as such, they are significant because they are the direct imprint of the processes that facilitate streaming flow. Hence, understanding the processes that form MSGLs is likely to provide insights into ice-stream flow mechanisms and the controls thereon.

Although the morphology of MSGLs and their significance as an indicator of streaming flow have been recognized for some time (Clark, 1993; Stokes and Clark, 1999), it is only recently that MSGLs have been observed beneath modern ice streams (King et al., 2009). The last decade has also seen the development of a number of divergent theories seeking to explain MSGL genesis (Clark et al., 2003; Schoof and Clarke, 2008; Shaw et al., 2008; Fowler, 2010).

* Corresponding author.
E-mail address: colm.ocofaigh@durham.ac.uk (C. Ó Cofaigh).

http://dx.doi.org/10.1016/j.quascirev.2013.06.028
0277-3791/

Clearly any attempt to fully understand MSGL formation and assess their role in ice stream dynamics is likely to benefit from observations of their internal structure and composition.

Given the logistical constraints of collecting such data from modern ice stream beds, the investigation of MSGLs associated with palaeo-ice streams provides a sensible target for assessing their mode(s) of formation. Perhaps surprisingly, however, observations of the internal sediment architecture and composition of MSGLs are relatively sparse, compared with drumlins (Stokes et al., 2011), and there have been only a few studies of MSGL sediments from terrestrially terminating ice streams (Lemke, 1958; Evans, 1996; Shaw et al., 2000; Stokes et al., 2008). These studies have all emphasised the contribution of subglacial reworking of pre-existing sediment depocentres during MSGL formation. Additionally, the last decade has seen observations of MSGL sedimentology from marine sediment cores collected from palaeo-ice stream beds on the Antarctic continental shelf (Wellner et al., 2001; Shipp et al., 2002; Dowdeswell et al., 2004; Ó Cofaigh et al., 2005, 2007; Evans et al., 2005; Reinardy et al., 2011). These studies have shown that MSGLs in these settings are typically composed of a weak, porous, subglacial till variously ascribed to subglacial sediment deformation or a combination of deformation and lodgement. Note, however, that because these cores represent point source samples and are spatially restricted, information on lateral facies variability and architecture is difficult to obtain from these types of data.

In this paper we report the results of a sedimentological investigation of MSGLs from along the course of the Finnie River, Nunavut, northern Canada (Figs. 1 and 2). The Finnie River is a tributary of the much larger Thelon River and, in places, flows perpendicular to the former flow direction of the Dubawnt Lake Palaeo-Ice Stream (Kleman and Borgström, 1996; Stokes and Clark, 2003; McMartin and Henderson, 2004). As a result it was targeted

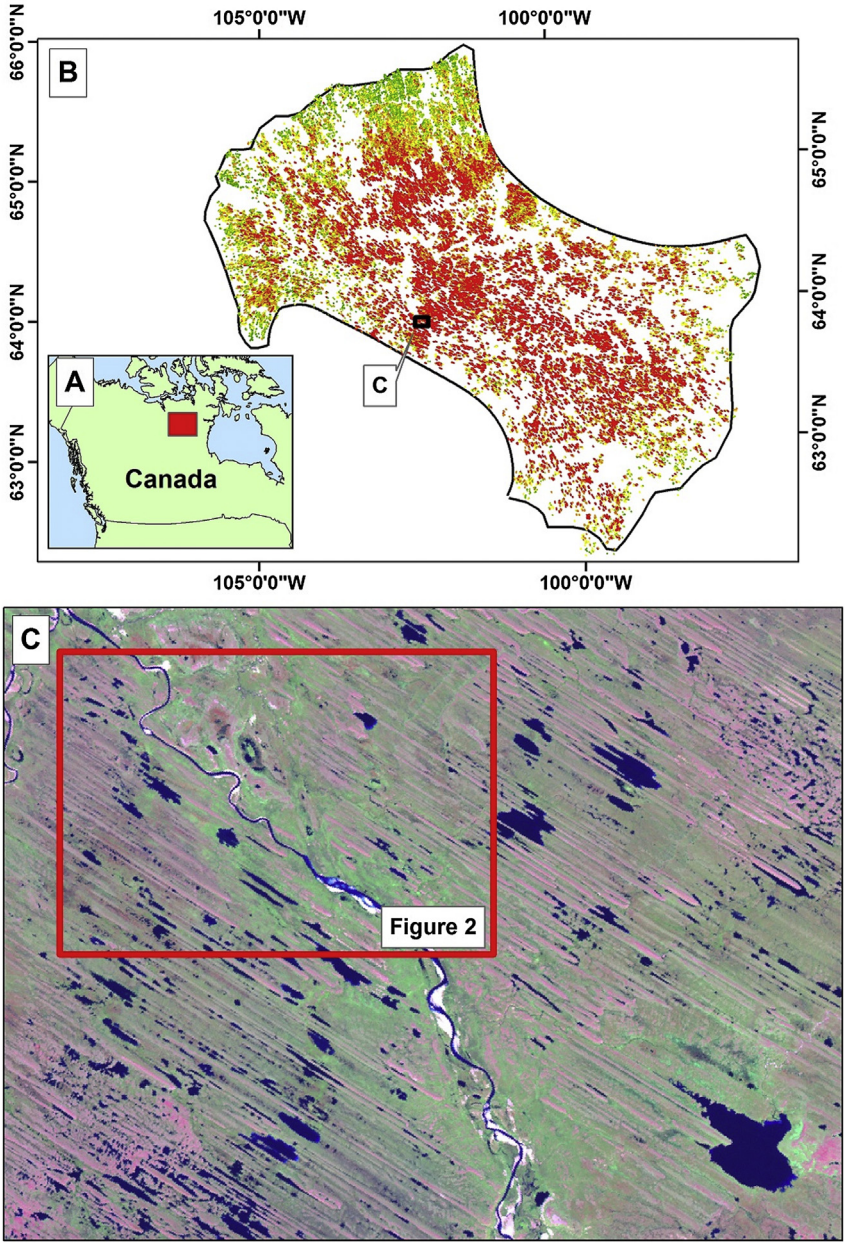

Fig. 1. Location map of the Dubawnt Lake Palaeo-Ice Stream flow-set (A), which contains over 40,000 glacial lineations (see Paper 1, Stokes et al., 2013), shown in (B) and coloured according to lineament length (green = < 500 m; red = > 1000 m). Landsat ETM image of the field area in the main trunk of the ice stream (bands 7,4,2: R,G,B) is shown in (C). (For interpretation of the references to colour in this figure legend, the reader is referred to the web version of this article.)

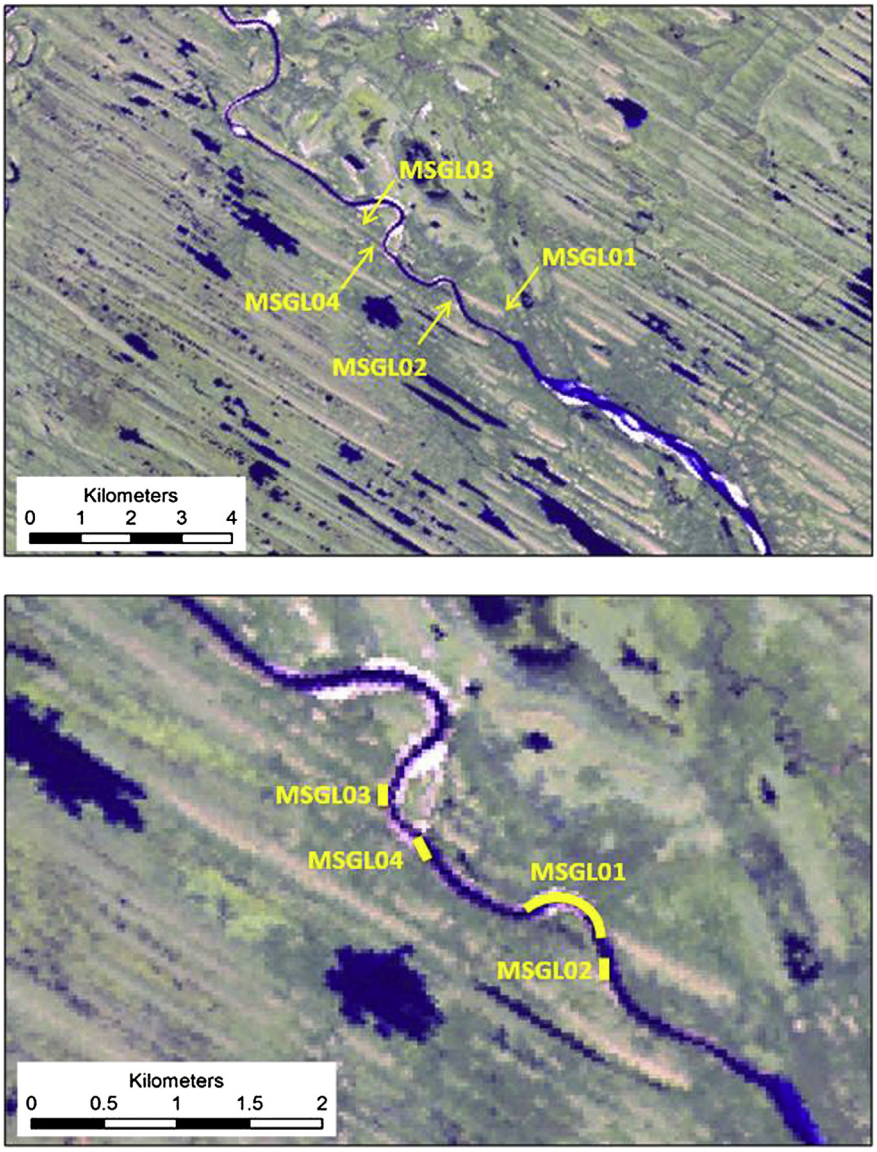

Fig. 2. Landsat ETM + satellite image of the study area (bands 7,5,1: R,G,B) showing the location of the subglacial bedforms (MSGL) (upper figure) and sections (lower figure) along the Finnie River, Nunavut.

to allow investigation of a number of sections through well-developed MSGLs in the central trunk of the ice-stream flow-set (Fig. 1), where velocities are assumed to have been highest (Stokes and Clark, 2003). This is the second paper emerging from an integrated study of the characteristics, morphology and internal composition of MSGLs on the bed of the Dubawnt Lake Palaeo-Ice Stream. The first paper focuses on analysis of the geomorphology (size, shape, and spacing) of a large sample of the landforms (Paper 1: Stokes et al., 2013), while the present paper focuses on their sedimentology and stratigraphy. The aims of this paper are to describe and interpret the sedimentology and stratigraphy of a series of MSGL ridges on the bed of the Dubawnt Lake Palaeo-Ice Stream and to discuss the wider implications of these data for MSGL genesis and sedimentary processes beneath ice streams.

2. Methods

Sections in MSGLs on the bed of the Dubawnt Lake Palaeo-Ice Stream are exposed as a result of fluvial incision along the present course of the Finnie River (Figs. 1 and 2). Fig. 2 shows a Landsat ETM + satellite image of the study area and the location of the sections reported in this study. The sites investigated were chosen purely on the basis of the availability and quality of sediment exposures in MSGL ridges. The stratigraphy and sedimentology of these exposures were examined during fieldwork in June 2006 and information on sedimentary structures, bed contacts, sediment body geometry, clast lithology, clast shape, texture and sorting was recorded. Section sketches and vertical graphic sedimentary logs were measured and recorded and all of these data were then used to characterize lithofacies (e.g. Figs. 3–5).

Clast macrofabrics were measured from the orientation and dip of the a-axis of clasts using $n = 50$ where possible (Fig. 6a). Comparisons are made with the a-axis and a-b plane macro-fabrics of previously studied subglacial tills sampled at modern glacier margins, subaqueous glacigenic diamictons and glacitectonites, utilizing the data presented by Benn (1994, 1995; Hicock et al., 1996; Evans and Hiemstra, 2005; Evans et al., 2007) (Fig. 6b and c). Hicock et al. (1996) devised the modality–isotropy diagram which plots isotropy (S_3/S_1) against values of fabric modality for various end-member till types of deformation, lodgement and melt-out. In

essence, this approach forces the researcher to visually assess the strength of a fabric and to use that assessment in conjunction with statistically derived fabric strengths based on eigenvalues (Fig. 6b). This is because eigenvectors calculated on bimodal or multimodal fabrics may be meaningless as they can lie between the actual fabric modes. More recently, Evans et al. (2007) re-plotted the modality–isotropy diagram using a/b plane data from glacigenic samples of known origin (Fig. 6b). Rather than using it to identify clear modality boundaries for specific till types as done by Hicock et al. (1996), Evans et al. used it to identify a clast fabric continuum that records the influence of lodged clasts in a range of subglacially deformed sediments. Both approaches are used in the present paper.

Assessment of clast roundness was undertaken on selected samples using the standard Power Roundness criteria and observations of surface features such as striations and facets were also recorded in order to assess the degree of modification (if any) by subglacial processes.

3. Stratigraphy and sedimentology

3.1. Results

Observations were primarily collected from exposures in four MSGL ridges along the course of the Finnie River (Figs. 2–4). In this region, the MSGLs are typically spaced at distances of 100–200 m apart, extend for several kilometres in length, and exhibit amplitudes of around 5–10 m (see also Paper 1: Stokes et al., 2013). The sections are orientated predominantly perpendicular or oblique to former ice flow as recorded by the lineation orientation. The four sites are labelled informally MSGL01-MSGL04 and are referred to as such throughout the rest of the paper (Fig. 2).

3.1.1. MSGL01

This section, located at 64° 2′ 19″N, 102° 23′ 54″ W, was the most extensive site investigated. It comprises a 10–12 m high, about 80 m wide section, cut obliquely through an MSGL ridge that records former ice flow to 299° (Figs. 2 and 3). Four logs (logs A, B, C and D) spaced 10–28 m apart were collected from across the section and together reveal a range of lithofacies (Fig. 4).

The lowermost unit consists of a consolidated, brown massive, matrix-supported diamicton (Figs. 3, 4 and 7b-f). The diamicton reaches a thickness of 4 m where Log B was recorded but this is likely a minimum as it disappears below the ground surface at the base of the section. It contains numerous striated and faceted clasts up to boulder size in a sandy silt matrix. Clasts are predominantly subrounded to subangular. Locally, the matrix varies from sandy zones to siltier (muddier) zones with the sandier zones corresponding to areas where the diamicton is more reddish-brown in colour. The diamicton appears to become more reddish-brown and sandier with depth so that there is an overall vertical change from a reddish brown sandy diamicton to siltier brown. The diamicton is notably fissile due to the presence of numerous subhorizontal partings spaced 3–8 cm apart and which can be continuous over distances of several tens of centimetres. Some of these partings are sandy and are less than 1 mm thick (Fig. 7b). In addition, the diamicton contains sandy lenses which are, in places, contorted (Fig. 7c). Clast a/b planes often lie parallel to the planes of the fissility. The upper contact of the brown diamicton is characteristically sharp and, at Log D (Figs. 4 and 7d), an inclined and tapered sand dyke penetrates downwards into the diamicton for 56 cm from the contact. The dyke tapers from 5 cm across at the top to less than 1 cm wide at its base.

Five clast macrofabrics were recorded within the brown diamicton (Table 1 and Figs. 3 and 6). All were taken from the centre of the diamicton but were spaced across section for a distance of 48 m. Fabric 1 (Table 1) had a moderate cluster and a mean lineation azimuth which dipped to the southwest; plotting this fabric on the modality–isotropy diagram shows that it is sub-bimodal and falls into the deformation till envelope (Fig. 6a and b). Fabrics 2 and 3 show moderately strong clusters with mean lineation azimuths which dip to the southwest and northeast. Both fabrics plotted in the lodgement/melt-out till envelope of the modality–isotropy plot of Hicock et al. (1996) and fabric 3 plots just outside the lodged clasts cluster on the fabric shape triangle (Benn, 1994) and on the modality isotropy plot of Evans et al. (2007) (Fig. 6). The final two clast macrofabrics from the brown diamicton (3 and 4; Table 1 and Fig. 6a) exhibited a relatively weak clustering (S_1 values of 0.581 and 0.517) dipping to the southwest. Both samples plot in the multimodal category of the isotropy-modality plot and in the deformation till envelope of Hicock et al. (1996) and low cumulative strain according to Evans et al. (2007) (Fig. 6b).

At Log A, the brown diamicton is overlain by 330 cm of poorly sorted, locally chaotic, sandy cobble-boulder gravel that is clast- to locally matrix-supported (Gm, Gms) with predominantly rounded-subrounded clasts (Fig. 4). The gravels are characterised internally by rapid vertical and horizontal variations in texture and contain contorted lenses of horizontally stratified, fine sand 10–30 cm thick. The gravels are overlain sharply by 1 m of ripple-drift, cross-laminated, fine sand (Type A). The rippled sands are contorted and faulted in places and they pinch out laterally across section. Where Log B was recorded (19 m northeast of Log A) the gravel and sand units above the brown diamicton thin to about 1–2 m and comprise contorted fine sand that in its lower 50 cm is amalgamated with the underlying brown silty diamicton. Further to the northeast, where logs C and D were recorded, the sand is not observed and the brown diamicton is overlain directly by red diamicton.

The red diamicton forms a continuous stratigraphic unit across section and thickens progressively to the northeast from 2.5 m,

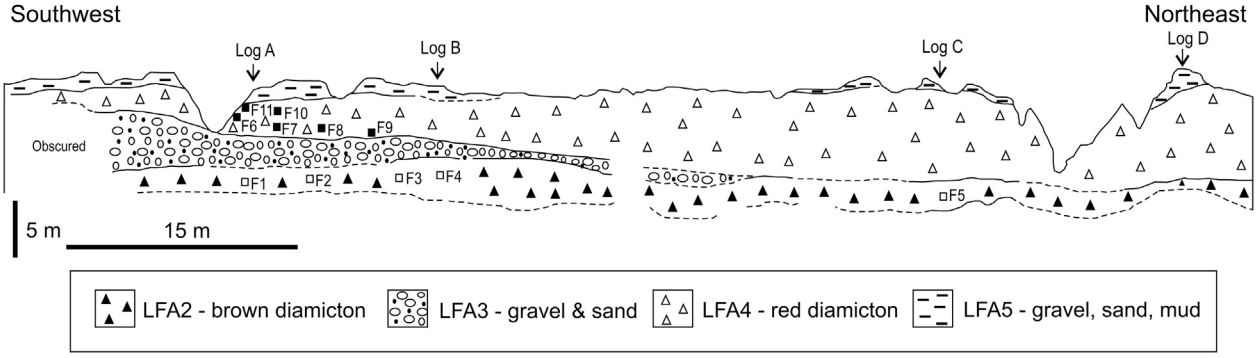

Fig. 3. Scaled drawing of the cliff section at MSGL01 showing vertical and lateral relationships between Lithofacies Associations (LFAs) 2, 3, 4 and 5, locations of the vertical profile logs shown in Fig. 4, and locations of fabric sites (F1-11; see also Table 1).

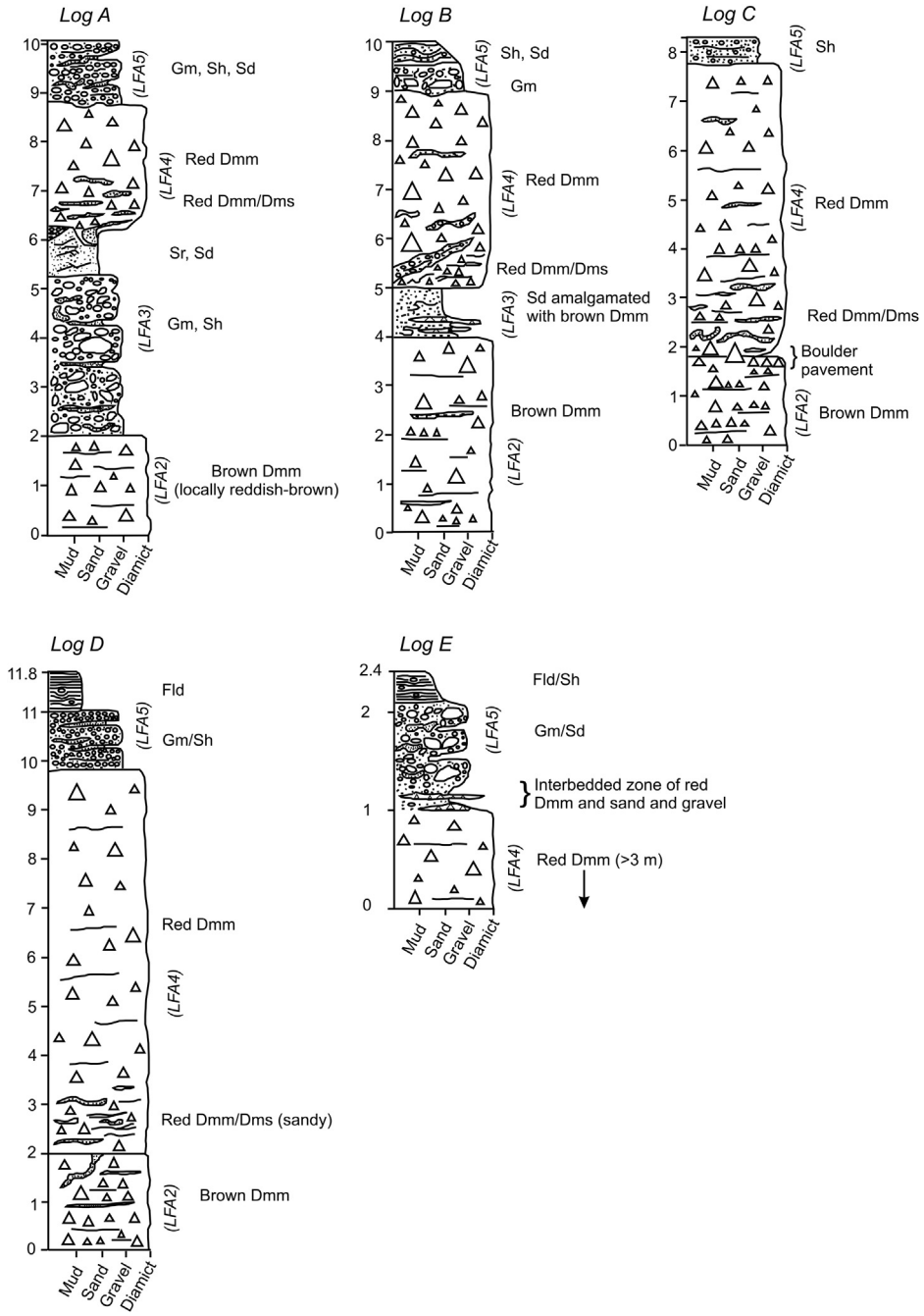

Fig. 4. Lithofacies logs from MSGL01. Log E was recorded from the upper part of the section 33 m to the southwest of Log A.

where Log A was recorded, to almost 8 m at Log D (Figs. 3, 4 and 8). The diamicton contains numerous striated and faceted clasts up to boulder size in a sandy matrix. Clasts range from rounded through to subrounded and subangular. Moving upwards, the red diamicton appears to become more poorly sorted (diamictic) with a greater proportion of clasts. Overall it is massive in structure (Dmm) but, in places, and particularly in the lower 1 m above its base, it is transitional to a stratified diamicton (Dms) due to the presence of numerous sandy stringers and lenses, which range from contorted to sub-horizontal, and which are similar in texture to the underlying sands (Fig. 8b, c and e). For example, where Log C was recorded, the lower ~60 cm of the diamicton is very sandy with numerous folded lenses and stringers of fine sand as well as gravelly pods, some of which are contorted. These 'sorted inclusions' range in thickness from 2 to 5 cm. Fissility is well developed locally. Where Log B was recorded, an attenuated bed of gravelly-outwash extends for 3.5 m into the red diamicton from the underlying gravels and sands (Fig. 4).

The lower contact of the red diamicton is characteristically sharp (Fig. 8b and h). In places (e.g., Log A), diamicton penetrates downwards into the underlying sand in a series of wedge-like dykes for 10–15 cm (Fig. 8d and f). These dykes bear similarities to the 'till wedges' described by Dreimanis (1992). They include tapered forms which extend downwards sub-vertically into the sands before becoming abruptly horizontal, and they appear to be attenuated, pinching out laterally across section. Elsewhere, the dykes are much more irregular and bulbous. In places, large clasts occur at the base of the red diamicton and protrude down into the

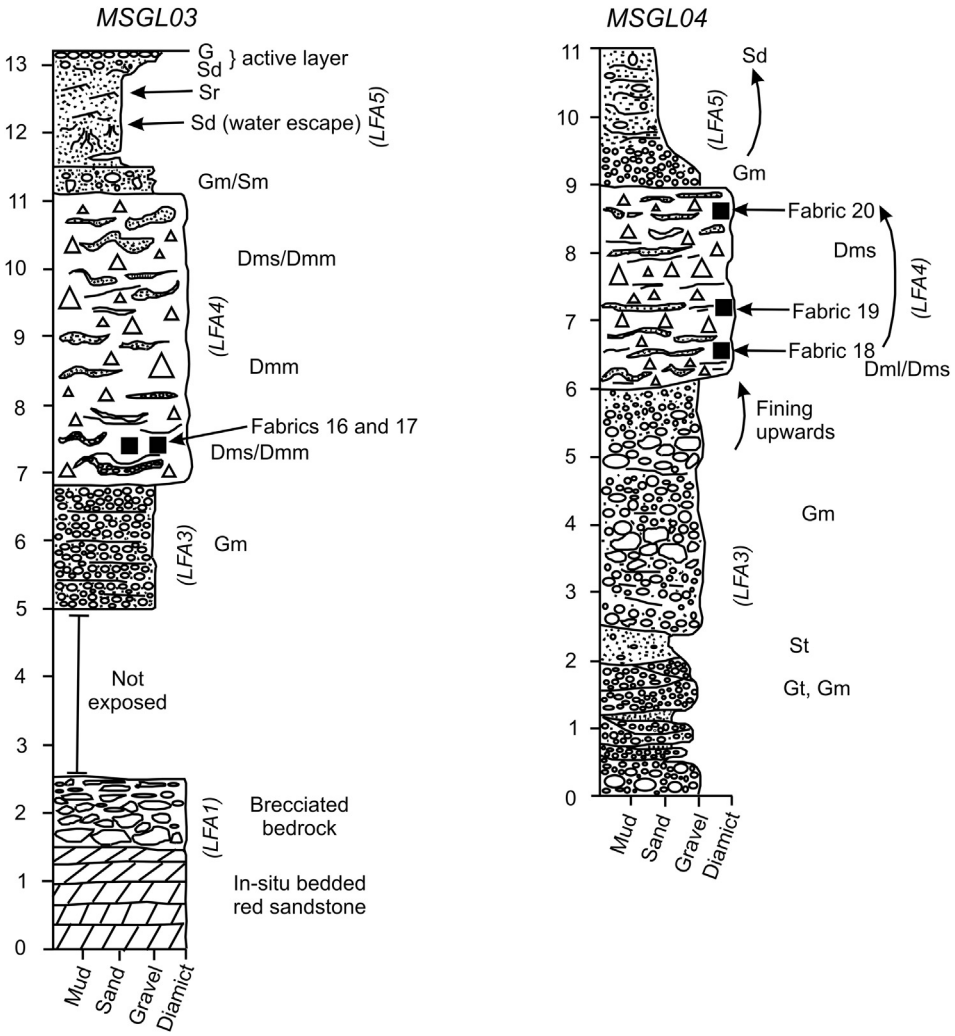

Fig. 5. Lithofacies logs from sites MSGL03 and MSGL04.

underlying sand (Fig. 8h). Laminae surrounding the lower parts of these clasts are contorted.

At logs C and D, the red diamicton rests directly on top of the lowermost brown diamicton and, where Log C was recorded, a crude boulder pavement extends for at least 2 m laterally along the contact (Figs. 4 and 7e). The boulders occur either at the base of the red diamicton, with their bases resting along the contact, or they occur at the top of the brown diamicton with their upper surfaces positioned at, or a few centimetres below, the contact with the red diamicton (Fig. 7e). Many of the clasts are planated, polished and striated on their upper surfaces (Fig. 7f) and they also include bullet-shaped forms with smooth and abraded stoss ends and plucked lee ends. Striae are typically orientated parallel to the long-axes of individual boulders and, in some cases, they wrap around the sides of the clast (Fig. 7f). In places, cross-cutting striae were observed, but these tend to be rare and the dominant striae direction is broadly parallel to the boulder long axis. The dominant dip direction of the boulders is to the northwest.

Six clast macrofabrics were recorded from the red diamicton across the section (Figs. 3 and 6 and Table 1). Fabrics 6-9 (Table 1) were collected over a lateral distance of 11 m. Fabric 9 (Table 1) was collected from 40 to 60 cm above the base of the red diamicton. Fabrics 7 and 8 (Table 1) were located 70 cm and 75 cm, respectively, above the lower contact; and Fabric 6 (Table 1) was located at 110 cm above the contact. Two further fabrics (10 and 11, Table 1) were recorded from 2 m above the base of the red diamicton, and within a few centimetres of the top contact of the red diamicton, respectively. All six fabrics showed relatively weak S_1 values that range from 0.434 to 0.588, with mean lineation azimuths that indicated dips to the northeast and southeast (Fig. 6a; Table 1). All six also plotted within the sub-bimodal and multi-modal categories on the modality–isotropy plot and thus within the low cumulative strain/deformation till envelopes (Hicock et al., 1996; Evans et al., 2007) (Fig. 6b). It should be noted that principal eigenvectors calculated on such modal classes may not be an accurate reflection of former ice flow direction as they may fall between actual fabric modes and this is certainly the case for fabrics 6, 8 and 11 (Fig. 6a and b; Table 1).

The section is capped by 1–2 m of bedded sand and gravel that exhibit considerable textural and structural heterogeneity and comprise 4 main facies (Figs. 3, 4 and 9). The complete sequence was recorded in the vicinity of Log A where directly overlying the red diamicton is up to 80 cm of ripple-drift, cross-laminated, fine sand (Type A ripples; Sr) (Fig. 9a). The sands contain dropstones that deform underlying laminae and are draped by overlying laminae. The rippled sands are overlain by parallel laminated fine sand (Sh), again with dropstones, and also containing lenses of diamictic gravelly material. The sands are interbedded with the top of the red diamicton over a thickness of a few tens of centimetres and grade up into about 80 cm of crudely bedded, clast- to matrix-

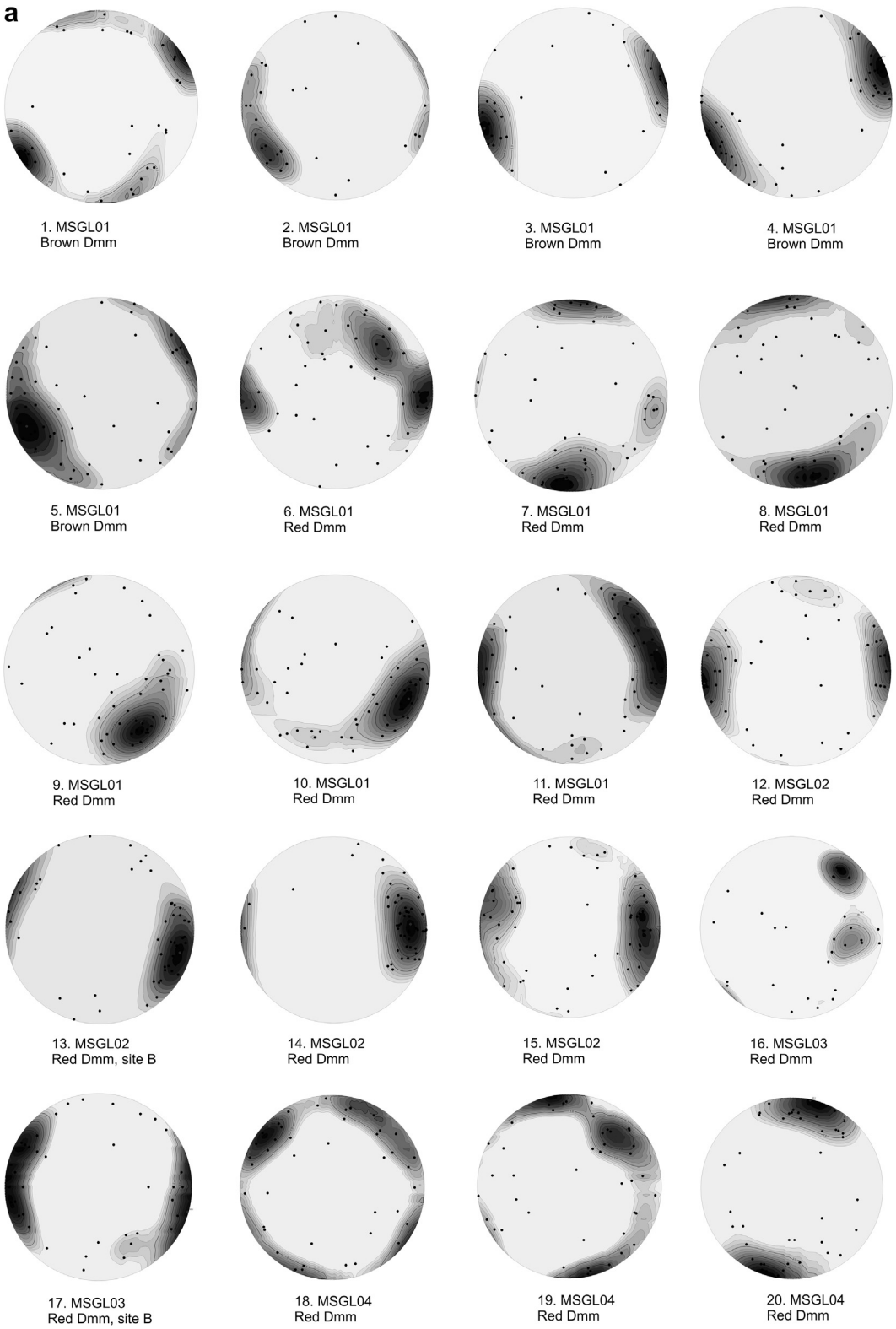

Fig. 6. Fabric data used in this study. (a) Clast macrofabric data from sites along the Finnie River plotted as lower hemisphere stereonets using the Rockware™ program and contoured using the Gaussian weighting factor. (b) Modality–isotropy plots of data from Finnie River, based on (i) Evans et al. (2007) and (ii) Hicock et al. (1996). The numbers refer to Table 1. Modality is assigned according to the Schmidt net plots and was constructed using the standard step function rather than the Gaussian weighting method used in Fig. 6a. Mm = multimodal to girdle like; sb = spread bimodal; bi = bimodal; su = spread-unimodal; un = unimodal. The envelopes shown in (i) contain data from deposits of known origin and shaded area represents that part of the graph in which stronger modality and isotropy in subglacial traction tills or glacitectonites reflects an increasing lodgement component. (c) Fabric shape triangle (after Benn, 1994) showing the fabric data from Finnie River used in this paper and control sample data for glacitectonite, subglacial till, lodged and ice-rafted clasts (Evans et al., 2007). Sample numbers refer to Table 1.

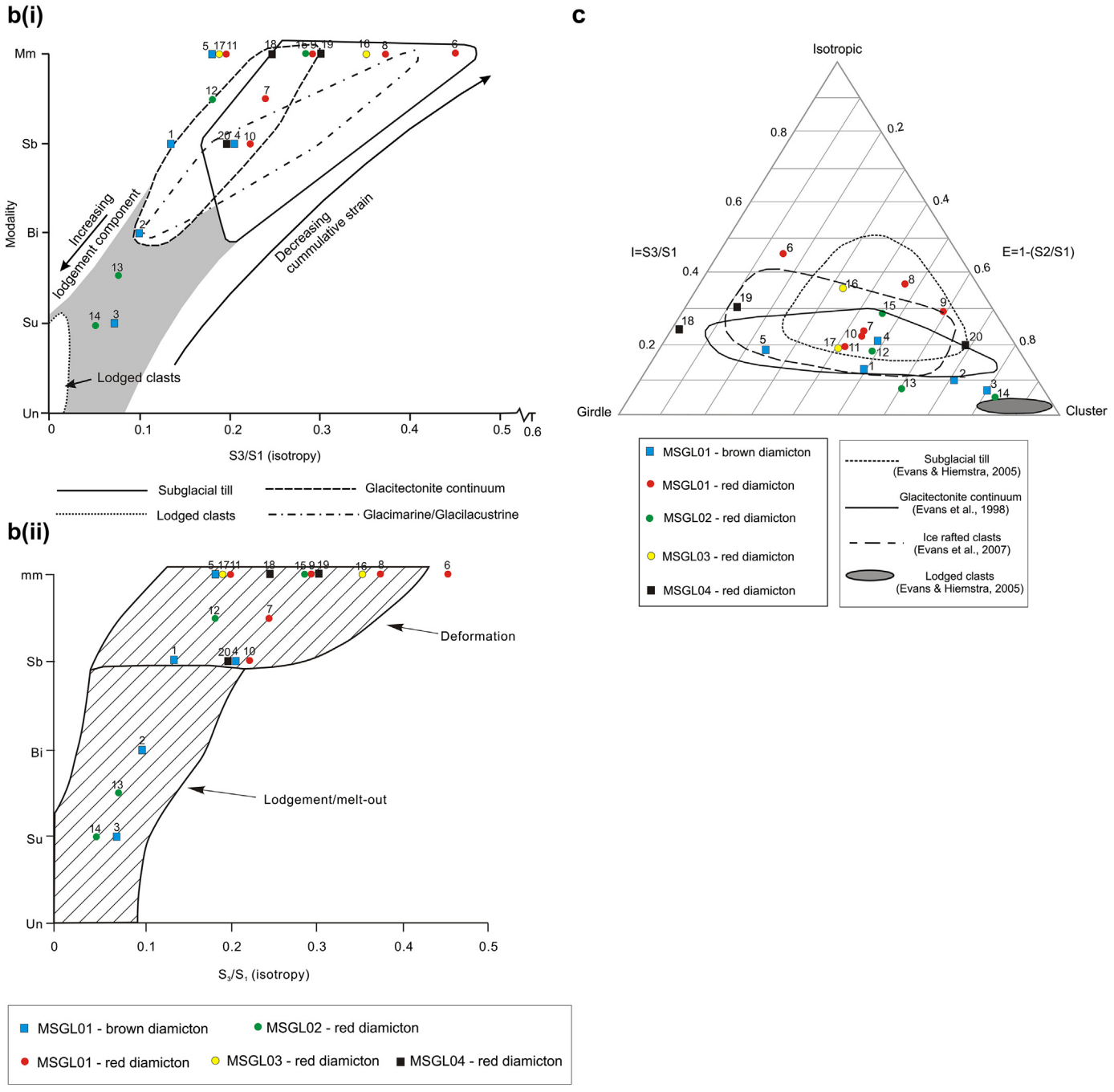

Fig. 6. (*continued*).

supported chaotic boulder to cobble gravel characterized by clast clusters, poor sorting, and pods of contorted laminated sand up to 10 cm thick (Figs. 4 and 9b and c). More commonly (logs A, B, D), the gravel rests directly on top of the red diamicton and is separated from it by an erosional, channelled contact. The gravels are overlain upwards by 30–100 cm of laminated, locally contorted, silty sand with dropstones (Fld) (Figs. 4 and 9d). The contact between the laminated silty sand and the underlying gravel is variable and ranges from gradational to sharp.

3.1.2. MSGL02

This site is located at 64° 2′ 9″N, 102° 23′ 52″ W (Fig. 2) and comprises a 2 m high section incised obliquely into the uppermost part of an MSGL ridge which records former ice flow towards the northwest (299°). The section comprises a red, sandy, matrix-supported, poorly consolidated, massive to stratified diamicton (Dmm-Dms) that, in places, is transitional to red silty sand. Pebble- to small boulder-size clasts occur throughout and many of the clasts are striated and subangular. The diamicton is at least 4 m thick at this site and contains rare stringers and laminae of sand (0.5–1 cm thick). Laminae range from undeformed to locally boudinaged.

Four clast macrofabrics were recorded in the red diamicton (fabrics 12, 13, 14 and 15; Table 1 and Fig. 6). Mean lineation azimuths varied strongly between the fabrics; fabrics 14 and 15 dip towards the east, while fabrics 12 and 13 dip to the west and southeast respectively (Table 1; Fig. 6). Assessments of fabric

Fig. 7. Details of lithofacies associations 1 and 2. (a) Breccia/clast supported diamicton with smudged bedrock clasts from base of MSGL03 (LFA1). (b–f) Details of the brown diamicton from MSGL01 (LFA2). (b) Massive matrix-supported diamicton with sandy stringers and dispersed clasts. Note sharp upper contact with overlying sand. (c) Matrix-rich largely massive diamicton with dispersed clasts up to cobble size and folded sandy lens. (d) The upper contact of the brown diamicton at Log D MSGL01 showing an inclined and tapered sand dyke which penetrates downwards into the diamicton for 0.56 m from the upper contact. (e) View taken along section in the vicinity of Log C MSGL01 showing a discontinuous crude boulder pavement formed at the contact between the brown (LFA1) and red diamictons (LFA3). The boulders are variably positioned either at the top of the brown diamicton with their contacts either at or a few centimetres below, the brown/red diamicton contact, or they occur at the base of the red diamicton with their bases resting along the contact. The boulders include bullet-shaped forms with smooth and abraded stoss ends and plucked lee ends. Striations on the boulders are typically oriented parallel to long-axes of individual boulders and in some cases wrap around the sides (f). (For interpretation of the references to colour in this figure legend, the reader is referred to the web version of this article.)

strength were similarly variable. Fabrics 13 and 14 both plotted outside of the subglacial till and glacitectonite envelopes on the fabric shape triangle but possess clustered fabrics and a modality–isotropy consistent with lodgement and meltout tills (Hicock et al., 1996) (Fig. 6b and c). Fabric 14, in particular, displays a strong cluster (S_1 value of 0.817). Fabrics 12 and 15 were weaker, but plotted within the subglacial till and glacitectonite envelopes and had a modality–isotropy similar to deformation till.

Table 1
Clast fabric statistics from sites along the Finnie River.

Fabric no.	Site	Facies	n	Mean lineation azimuth	S_1	S_2	S_3	S_3/S_1	Modality
1	MSGL01	Brown Dmm	30	252.6	0.612	0.309	0.079	0.129	sb
2	MSGL01	Brown Dmm	30	254	0.723	0.207	0.07	0.097	bi
3	MSGL01	Brown Dmm	50	62.4	0.786	0.157	0.057	0.072	su
4	MSGL01	Brown Dmm	50	246.3	0.581	0.298	0.121	0.208	sb
5	MSGL01	Brown Dmm	32	215	0.517	0.39	0.093	0.180	mm
6	MSGL01	Red Dmm	50	73.9	0.434	0.369	0.197	0.454	mm
7	MSGL01	Red Dmm	50	175.2	0.556	0.311	0.132	0.237	sb-mm
8	MSGL01	Red Dmm	50	167.8	0.525	0.281	0.194	0.369	mm
9	MSGL01	Red Dmm	50	141.2	0.588	0.24	0.172	0.292	mm
10	MSGL01	Red Dmm	54	112	0.562	0.313	0.125	0.222	sb
11	MSGL01	Red Dmm	52	77.3	0.563	0.328	0.109	0.194	mm
12	MSGL02	Red Dmm	50	262.3	0.592	0.302	0.106	0.179	sb-mm
13	MSGL02	Red Dmm	50	106.2	0.68	0.269	0.051	0.075	bi-su
14	MSGL02	Red Dmm	50	85.8	0.817	0.141	0.042	0.051	su
15	MSGL02	Red Dmm	50	91.1	0.547	0.297	0.156	0.285	mm
16	MSGL03	Red Dmm	30	78.9	0.494	0.329	0.176	0.356	mm
17	MSGL03	Red Dmm	43	105.5	0.561	0.333	0.106	0.189	mm
18	MSGL04	Red Dmm	43	314.4	0.45	0.441	0.109	0.242	mm
19	MSGL04	Red Dmm	43	45.1	0.458	0.403	0.139	0.303	mm
20	MSGL04	Red Dmm	43	11.8	0.663	0.206	0.131	0.198	sb

Mm = multimodal to girdle like; sb = spread bimodal; bi = bimodal; su = spread-unimodal.

3.1.3. MSGL03

This site is located at 64° 2′ 43″N, 102° 25′ 39″ W. It is a 13 m high section, facing west, that is cut obliquely into an MSGL ridge and consists of a range of lithofacies (Fig. 5). The section rests on 1.5 m of *in-situ* sandstone bedrock and is poorly exposed in its lower 5 m. The *in-situ* bedrock is gradationally overlain by 1 m of brecciated sandstone (Dcm). Brecciation comprises numerous, angular, sandstone clasts and increases upwards. In its uppermost 40 cm, clasts are pulverized and many are 'smudged' (Figs. 5 and 7a). The overlying 2.5 m is obscured by slumped material and the slumped section is overlain by 170 cm of massive, clast-supported, well sorted pebbly gravel with rounded clasts (Gm) (Fig. 5).

The gravel is overlain sharply by 430 cm of poorly consolidated, red diamicton ranging from massive to stratified (facies Dmm, Dms) and comprising subrounded to subangular, striated and facetted clasts up to small boulder size in sandy matrix (Fig. 5). Texturally, the matrix ranges from fine sand to silty sand and it has a 'chaotic' or contorted appearance with rapid vertical and lateral transitions from zones of well sorted fine sand to more diamictic, poorly sorted sand. Towards the base of the diamicton, contorted inclusions of pebbly gravel are visible but, more commonly, inclusions are mainly sandy and take the form of numerous contorted sandy pods and lenses up to about 15 cm thick which can extend laterally for several tens of centimetres.

Two clast macrofabrics were collected 40–80 cm below the upper contact of the red diamicton (16 and 17; Table 1; Fig. 6). Both are relatively weak (S_1 values of 0.494 and 0.561) and dip to the ENE and ESE respectively (Fig. 6a). They plot in the deformation till zone of the modality–isotropy plot of Hicock et al. (1996) and in the multi-modal range of Evans et al. (2007) (Fig. 6b) suggesting they have been subjected to relatively low cumulative strain.

The red diamicton is overlain by 45 cm of poorly sorted, massive, sandy pebble gravel (Gm) that is predominantly matrix-supported and contains occasional subrounded to subangular clasts up to cobble size. The contact between the gravel and underlying red diamicton occurs over a vertical thickness of about 5 cm and is represented by an upward change in texture and colour. The pebbly gravel is overlain by 130 cm of rippled fine sand and silty sand. Palaeocurrent measurements indicate flow to 302°. The lower 30 cm of the unit comprises bedded silty sands which are contorted and have upturned and broken laminae characteristic of water escape.

The uppermost 40 cm of the exposure is a heavily disturbed zone of fine sands with occasional clasts and rootlets and likely represents the active layer. The section and overlying ground surface is capped by a thin (10 cm) gravelly lag.

3.1.4. MSGL04

This site is located at 64° 2′ 27″N, 102° 25′ 17″ W. It comprises an 11 m high section, facing 06°, and is cut obliquely into a single MSGL ridge which subsequent postglacial gullying has further incised (Figs. 2 and 8a). The MSGL ridge records a former ice flow direction of 299°.

The lowest 6 m of the sequence comprises texturally heterogeneous, variably stratified and sorted gravel beds with minor sandy units (facies Gm, minor Gms, Gp, Sh, Sm). In the basal 2.5 m, the sediments consist of cross-cutting beds of cobble-pebble gravel with occasional sandy interbeds of coarse-fine sand that are internally crudely stratified to massive (facies Gm, Sh). Individual beds tend to be lenticular in their geometry. Clasts within gravel beds appear to be predominantly subrounded, although some rounded and subangular clasts were also recorded. Individual beds are 20–50 cm thick and are variably sorted, ranging from well sorted, clast-supported pebble gravel to beds containing a greater proportion of matrix in which the larger clasts are set in a coarse sandy to granule matrix. Bedding contacts are variable and range from well defined and abrupt to more gradational, where the contact is defined by upward changes in sorting and/or grain size. Occasional zones of imbrication are observed within some individual gravel beds. Imbrication is of the b-axis imbricate/a-axis transverse type. These bedded gravels coarsen upwards into 2 m of clast- to locally matrix-supported cobble-small boulder gravel (Gm). Individual beds are very poorly defined and primarily result from subtle gradational changes in grain size and sorting. Clasts are predominantly subrounded with b(i) a(t) imbrication observed. These coarse gravels fine upwards into 1 m of well sorted, clast-supported pebble gravel which, in turn, fines upwards crudely to the contact with the overlying red diamicton.

The gravels are overlain by 3 m of sandy, poorly-consolidated, red, matrix-supported, stratified diamicton (predominantly Dms but towards the base Dml). The contact with the underlying gravels is very sharp and is also marked by an abrupt colour change (Figs. 5 and 8a). The diamicton contains numerous striated and faceted clasts up to small boulder size in a sandy matrix. Clasts are

Fig. 8. Details of lithofacies associations 3 and 4. (a) Photo of MSGL04 sections. Note the sharp planar contact between gravels of LFA3 and overlying red diamicton of LFA4. (b–h) Details of the red diamicton (LFA4) from MSGL01 and MSL04 and especially the nature of its contact with the underlying outwash of LFA3. (b) Sharp erosional contact between the red diamicton of LFA5 and the underlying sand, MSGL01. Note the stringers of sand within the lower few centimetres of the diamicton. Twenty centimetres of diamicton are shown in the photo. (c) The base of the red diamicton with about 15 cm of sand (LFA3) below around the level of the trowel handle, MSGL01. The contact between the diamicton and sand is irregular and 'mixed' with contorted sandy stringers and lenses present in the base of the diamicton. (d) Contact between the red diamicton and underlying sand of LFA3, MSGL01. Note the presence of diamicton dykes which penetrate downwards into the sand from the diamicton above and become abruptly horizontal. (e) Mixed zone of sandy red diamicton with contorted sand lenses and crudely imbricated cobble clasts in the diamicton, MSGL01. (f) deformed mixed zone of sand and overlying red diamicton, MSGL01. The red diamicton appears to have penetrated downwards into, and become partially mixed with, the underlying sand. (g) Detail of the red diamicton facies association in MSGL04. Note the stratified nature with dispersed clasts in a very sandy matrix. The stratification is crude and is imparted by sandy lenses and horizons which are laterally discontinuous across the section. In places this material is transitional to deformed poorly sorted sand rather than sandy diamicton. (h) Contact between the red diamicton and underlying sands of LFA3, MSGL01. The photos shows a small boulder which protrudes from the base of the diamicton into the sand. (For interpretation of the references to colour in this figure legend, the reader is referred to the web version of this article.)

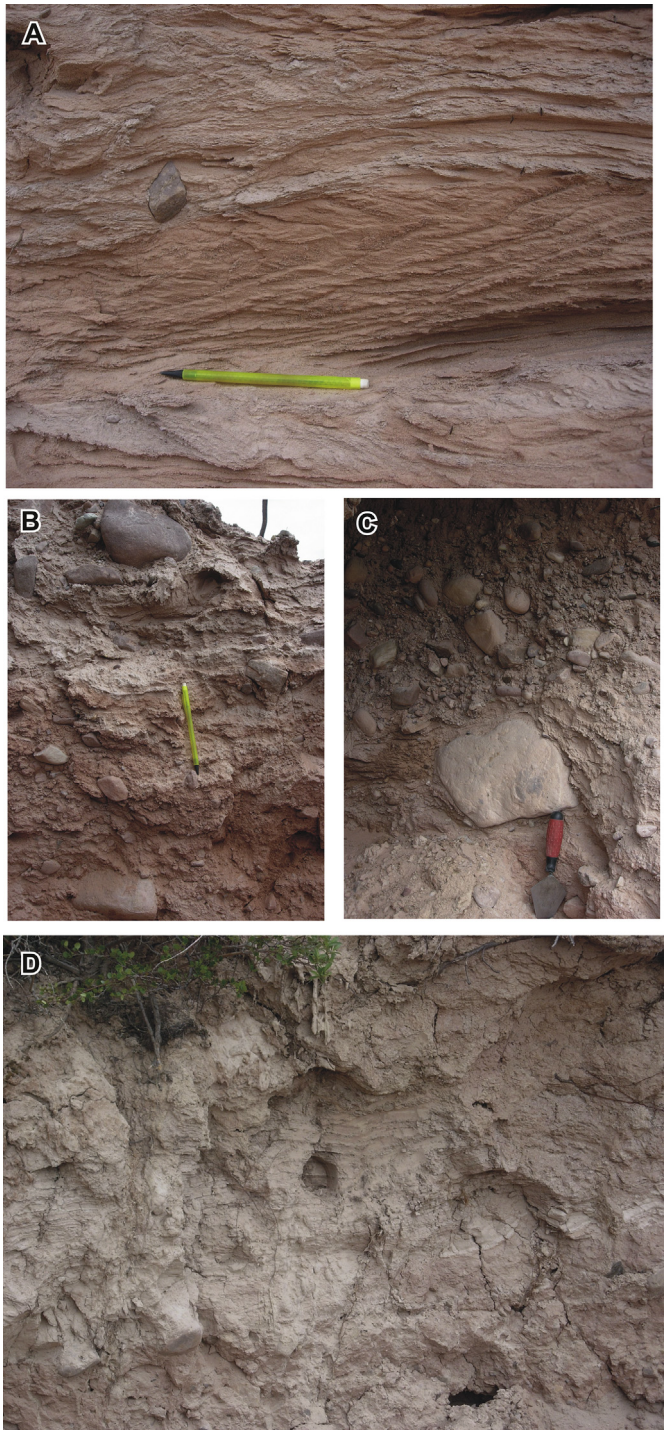

Fig. 9. Details of Lithofacies Association 5 (glacilacustrine sediments) from MSGL01. (a) Ripple-drift cross laminated sands (Type-A) with an isolated dropstone. (b) Poorly sorted, crudely bedded, pebbly gravel with occasional outsized cobble-small boulder lonestones overlain by contorted bedded sands with lonestones up to small boulder size which are interpreted as a product of ice-rafting; (c) The lower 20 cm of the section comprises laminated pebbly sand with a large outsized dropstone. Note the deformed laminations above and below the clast. The sands are overlain sharply by massive poorly sorted clast-matrix supported cobble-small boulder gravel; (d) Laminated silty sand that is locally contorted and contains occasional dropstones up to cobble size.

subrounded to subangular. In general, stratification is imparted by the presence of numerous sandy and gravelly stringers, pods and lenses that range in thickness from 2 to 10 cm and which, in places, contain faint lamination. The lowermost 50 cm of the diamicton is stratified to laminated, matrix-supported (Dms-Dml) and is transitional to poorly sorted sand with gravel clasts (Fig. 8g). Sandy lenses are texturally diverse, ranging from fine to coarse, and some are internally laminated with, locally, current ripples preserved and un-deformed laminae over vertical thicknesses of 5–10 cm. In its uppermost 40–50 cm, the diamicton is stratified with stratification imparted by the presence of sandy lenses up to 10 cm thick and laminated zones which are laterally continuous over at least 50 cm across section. The lenses are visible on account of variations in texture and colour, with transitions from red through to white through to silty white sand.

Three clast macrofabrics were collected from the red diamicton (Table 1 and Fig. 6). The two lower fabrics were collected from 60 cm to 120 cm, respectively (18 and 19; Table 1), from above the contact with the underlying gravels. These are weak (S_1 values of 0.45 and 0.458) with mean lineation azimuths of 314° and 45° (Table 1 and Fig. 6). Both fabrics possess a multi-modal modality–isotropy signature plotting in the deformation till and subglacial till/glacitectonite envelopes of the modality–isotropy plot (Fig. 6b) (Hicock et al., 1996; Evans et al., 2007), but plotting outside of these envelopes on the fabric shape triangle (Fig. 6c). A final clast macrofabric was recorded from 20 to 40 cm below the upper contact (20, Table 1; Fig. 6). This displayed a moderately strong clustering (S_1 values of 0.663) and a mean lineation azimuth of 11.8°. Analysis of fabric strength reveals that the uppermost sample possesses a strain signature similar to subglacial till/glacitectonite and a modality–isotropy in the subglacial till-glacitectonite envelopes (Fig. 6b).

The diamicton is overlain sharply by 60 cm of bedded pebbly gravel, which grades upwards into 140 cm of contorted, whitish silty sand with rare cobble-sized lonestones (Sh, Fld).

3.2. Lithofacies Associations

Based on the observations from section exposures at the four sites, we define five lithofacies associations (LFAs).

3.2.1. Lithofacies association 1

LFA1 was only observed in MSGL03 (Fig. 5). It comprises the sandstone breccia (Dcm) which rests on *in situ* sandstone bedrock at the base of the section. Brecciation increases vertically upsequence and the top of LFA1 comprises pulverized and smudged bedrock.

3.2.2. Lithofacies association 2

LFA2 (brown diamicton; Dmm) was only exposed in MSGL01 where it forms the basal unit of the stratigraphic sequence (Figs. 3 and 4). It consists of a brown to reddish-brown, massive, matrix-supported, fissile diamicton with numerous striated and facetted clasts in a silty matrix. It contains rare contorted sandy lenses. Clast macrofabrics are variable in strength. Fabrics 1, 2 and 3 have S_1 values of 0.612–0.786 but fabrics 4 and 5 are relatively weak with S_1 values of 0.581 and 0.517, respectively. With the exception of fabric 3 which dips to the northeast, the other four fabrics measured within the brown diamicton dip southwest, which is perpendicular to the regional ice flow direction inferred from the MSGL long-axes.

3.2.3. Lithofacies association 3

LFA3 (gravel and sand; Gm, Gms, Gp, Sh, Sr, Sm) is exposed in MSGL01, MSGL03 and MSGL04 (Figs. 3–5). It comprises a gravel and sand association that is dominated by crudely bedded to well stratified gravel up to boulder size, with occasional massive units with minor interbeds and lenses of horizontally laminated, rippled and massive sands. A characteristic feature of LFA3 is the rapid

vertical and lateral variation in texture, sorting and matrix. Sandy lenses are interbedded within the gravels but are typically laterally discontinuous. Where imbrication is observed in gravel beds it is the a(t) b(i) type. Bed contacts range from sharp, to gradational in which the boundary is marked by gradual changes in grain size over several centimetres or more. At MSGL01 LFA2 displays a vertical transition from the coarse, poorly sorted gravelly facies into well sorted, ripple-drift, cross-laminated sand that is in places contorted and penetrated by wedges or dykes of diamicton from the overlying red diamicton of LFA3.

3.2.4. Lithofacies association 4

LFA4 (diamicton; Dms, Dml, Dmm; transitional in places to poorly sorted Sd with clasts). LFA4 comprises the red sandy diamicton facies that crops out in all sections investigated along the Finnie River (Figs. 3–5). It is matrix-supported and ranges from massive to stratified with numerous striated and facetted clasts. Stratification is particularly common in the lower part of the diamicton due to the presence of numerous lenses, stringers and pods of sand and, in places, gravel. These sorted layers are, in places, contorted. Toward the base of the red diamicton, the sandy inclusions can be sufficiently abundant that the diamicton has a crudely laminated appearance (facies Dml). In some places, the sorted sediments can also be seen to have been thrust and attenuated into the lower part of the red diamicton. The lower contact of LFA4 with the underlying outwash of LFA3 is, invariably, sharp, and sediments of LFA3 directly beneath the contact are in places deformed. At MSGL01, dykes of the red diamicton taper downwards into LFA3 before becoming abruptly sub-horizontal and attenuated (Fig. 8). Clast macrofabrics within LFA4 are overwhelmingly subbimodal or multimodal and fall into the deformation till envelope of Hicock et al. (1996). The exceptions are fabrics 13 and 14 from MSGL02 which are strong (S_1 values of 0.68 and 0.817) and plot in the lodgement-meltout till envelope (Fig. 6).

3.2.5. Lithofacies association 5

The uppermost lithofacies association (LFA5; gravel, sand, mud association; Gm, Sr, Sh, Sd, Fld) typically sharply overlies LFA4 and is both texturally and sedimentologically heterogeneous (Fig. 4). Facies within LFA5 comprise poorly-sorted, crudely-bedded, clast- to matrix supported gravel with contorted interbeds of laminated sand and clast clusters, ripple-drift cross-laminated (Type A) and horizontally laminated sands with dropstones, and laminated silty sand with dropstones. The latter facies comprises the uppermost stratigraphic unit recorded in the study area.

3.3. Interpretation

The stratigraphy and sedimentology observed at the four sites are now interpreted according to the five lithofacies associations (LFAs) described above.

3.3.1. LFA1 (clast-rich diamicton and breccia association)

LFA1 was only observed at the base of MSGL03. The sandstone breccia rests directly on *in-situ* sandstone bedrock and brecciation increases up-sequence, with individual clasts becoming gradationally more disaggregated and the top of the LFA consisting of pulverized and smudged bedrock. These characteristics are consistent with an interpretation of LFA1 as a glacitectonite formed by the subglacial quarrying and entrainment of sandstone bedrock blocks followed by their pulverization and comminution during subglacial transport (cf. Croot and Sims, 1996; Hiemstra et al., 2007; Lian and Hicock, 2010). Bedrock liberation and entrainment would have been facilitated by the weak sandstone bedrock which would have been displaced along joints and bedding planes to form rafts that were then incorporated prior to being crushed subglacially.

3.3.2. LFA2 (brown diamicton association)

This LFA crops out only in MSGL01, where it forms the lowermost stratigraphic unit recorded at the section. Based on its poorly sorted texture, well developed fissility, the presence of contorted sandy inclusions within the diamicton matrix, as well as striated and faceted clasts, the brown diamicton of LFA2 is interpreted as a subglacial till (Evans et al., 2006). The dominant dip direction to the southwest recorded by four out of the five fabrics suggests that the brown diamicton was deposited by an ice flow from that direction which, as noted above, is perpendicular to the regional ice-flow direction during deglaciation, as recorded by the ice-stream flow set MSGLs (Fig. 1). The northeast dip recorded in fabric 3 from this site is difficult to reconcile with ice flow from the southwest, which has not been recognized in previous studies, although it is possible that it reflects fabric reorientation due to the localized influence of topography.

The fabrics from the brown diamicton are variable in terms of fabric strength and modality—isotropy, with some fabrics being multimodal or sub-bimodal and plotting in the deformation till envelope of the modality isotropy plot (Fig. 6b). Others clast fabrics from the brown diamicton were more clustered and sub-unimodal or bimodal, and plotted in the lodgement/meltout envelope (Hicock et al., 1996; Evans et al., 2007) (Fig. 6b). These data are consistent with the brown diamicton being a form of 'hybrid till' formed by a combination of lodgement and deformation (Hicock and Fuller, 1995; Lian and Hicock, 2000, 2010; Nelson et al., 2005; Evans et al., 2006). Evans et al. (2006) have used the term 'subglacial traction till' to refer to such deposits.

The brown till is undated and was recorded only in MSGL01. Extensive reconnaissance along the Thelon River in 2004 and 2005, which spans over 200 km of the former ice stream bed to the north and east, failed to observe this brown till in any other location (see also Stokes et al., 2008). Given its sporadic nature and the fact that the fabric orientations are aligned perpendicular to the west/northwestward post-LGM ice flow directed by the Keewatin Ice Divide (Dyke and Prest, 1987) this till could have been deposited either at the LGM and several thousand years prior to the initiation of the ice stream or alternatively it records a pre-LGM ice flow. We note that the south-west to north-east orientation of the fabrics is consistent with the orientation of patches of degraded and 'anomalous' lineation patterns within Keewatin that Kleman et al. (2010) suggest record pre-LGM ice flow from a dispersal centre to the NE of our study region. Thus, it is possible that the brown till is associated with these pre-LGM ice flows. However, and as noted above, the majority of the fabric data point to ice flow from the south-west in this particular location, rather than the NE. It is difficult to reconcile a NE flow towards the location of a major ice divide (the Keewatin Ice Divide) that persisted throughout the last deglaciation and so we speculate that this till most likely relates to a pre-LGM flow. However, flow towards the NE has not been reported in this region of the LIS and thus the age of the till and the associated ice flow direction must remain necessarily speculative in the absence of dating control and till geochemistry from the site.

3.3.3. LFA3 (gravel and sand association)

The texturally variable sediments of LFA3 record sedimentation in a largely glacifluvial sandur-type depositional environment (Boothroyd and Ashley, 1975; Miall, 1992). Massive, crudely bedded and well stratified gravels containing clasts up to boulder size formed through the aggradation and migration of braid bars in a relatively proximal sandur setting. Bedload transport is supported by the presence of a(t) b(i) imbrication within the gravels which

indicates rolling and saltation of clasts along the bed. Discharge appears to have been pulsatory based on the lateral and vertical variations in texture within the gravel units. Finer-grained, sandy lenses interbedded with the gravels likely represent deposition in abandoned channels. At MSGL01, the stratigraphic sequence exhibits an overall fining-upwards trend with the gravels overlain by ripple-drift, cross-laminated sand. This vertical fining upwards transition is interpreted to record aggradation followed by a gradual waning of flow and channel/bar migration across the sandur.

3.3.4. LFA4 (red diamicton association)

LFA4 comprises a massive to stratified (in places laminated), matrix-supported, sandy diamicton that is red in colour. In places, it is transitional to deformed sand. Stratigraphically, it overlies the outwash of LFA3 and forms a distinctive unit within the MSGLs of the study area. Observations from elsewhere on the former ice-stream bed support the interpretation that this red diamicton is intimately associated with landforms produced by the ice stream (Stokes et al., 2008). This interpretation is also supported by studies of till composition and stratigraphy from the Thelon River/Schultz Lake region west of Chesterfield Inlet. There, McMartin et al. (2006) show that the surficial till located inside the limits of the Dubawnt Lake Ice Stream has a reddish-pinkish coloured matrix reflecting a high proportion of Dubawnt lithologies transported westwards from the Baker Lake Basin. Surficial tills from outside the north-eastern margin are olive brown to grey brown in colour reflecting a dominance of supercrustal and/or intrusive clasts (McMartin et al., 2006). Thus the reddish till appears to be strongly related to the ice stream pathway, although given the evidence for earlier flow phases and shifts in the position of the Keewatin Ice Divide from this region (e.g., Aylsworth and Shilts, 1989; McMartin and Henderson, 2004) we cannot rule out the possibility that some of the till is at least partially related to earlier flow phases.

The characteristics of LFA4 are consistent with a subglacial origin by overriding, incorporation, and subglacial reworking of the sand and gravel of LFA3. Evidence for this includes attenuated rafts of outwash within the diamicton; numerous lenses and stringers of sand, many of which are deformed; an upwards transition from crudely laminated to stratified diamicton or from stratified to massive diamicton that suggest increased transport and mixing toward the top of the unit; a typically sharp, erosional lower contact with LFA3, and deformation of this underlying outwash. Also present are dykes and injections of red diamicton which penetrate downwards into LFA3 and show horizontal displacement and attenuation. The sandy texture of the red diamicton reflects the parent material from which it is derived, namely the outwash of LFA3. The well preserved nature of many of these lenses and rafts implies a relatively short transport distance and low cumulative strain (Banham, 1977; Benn and Evans, 1996; Ó Cofaigh et al., 2011), an interpretation also supported by the fact that the diamicton is, in places, transitional to deformed sand.

At MSGL01, where logs C and D were recorded, the glacifluvial outwash of LFA3 is absent and, instead, the red diamicton directly overlies the basal brown diamicton of LFA2. This absence may reflect the erosion and removal of LFA3 at these sites during emplacement of the red diamicton, although the sands and gravels do appear to thin laterally across section from logs A and B (Fig. 2). The boulder pavement along the contact comprises a series of striated, planated and polished clasts (Fig. 7e and f). As noted above, some of the pavement boulders rest directly on the contact whereas others occur just below it, in the top of the brown diamicton, with their upper surfaces either along the contact or a few centimetres below it.

There are a number of different interpretations of clast pavements in subglacial tills, ranging from lag deposits formed by erosion (subglacial winnowing) at the ice-bed interface and removal of the surrounding matrix resulting in the concentration of the larger clasts (Boyce and Eyles, 2000; Jørgensen and Piotrowski, 2003), to the sinking of large clasts through a deforming till layer (Clark, 1991), to local accumulation as a result of lodgement (Boulton and Paul, 1976), to a combination of lodgement, deformation and melt-out with subsequent abrasion and striation of the upper surfaces of the clasts (Hicock, 1991). We suggest that the characteristics of the boulder pavement at MSGL01 are consistent with an origin by a combination of lodgement and abrasion as well as the downward erosion of the brown till matrix and resulting concentration of clasts. Lodgement is suggested by the clasts at the base of the red diamicton whose lower surfaces are positioned at the contact with the brown diamicton and whose upper surfaces are striated and planated. Sinking of the clasts through a deforming sediment layer would be more likely to have resulted in clast rotation and the formation of multiple cross-cutting striae both parallel and transverse to the long axis. Although some cross-cutting striae were observed, more generally, striae tend to be orientated broadly parallel to the long axis. Hence, we do not consider clast sinking through a deforming weak sediment matrix to be the major process forming the clast pavement. Clasts with striated upper surfaces also occur in the upper part of the brown diamicton and a few centimetres below the contact; characteristics which suggest winnowing of the matrix and abrasion by overriding ice (cf. Davies et al., 2009).

Clast macrofabrics from the red diamicton are typically weak with S_1 values ranging from 0.4 to 0.5 and the majority of fabrics being multimodal and plotting in the deformation till envelope on the modality isotropy plot (Fig. 6), which suggests that they were subject to relatively weak cumulative strain. However, in MSGL02, several clast macrofabrics from the red diamicton are considerably stronger (S_1 values of 0.6–0.8), suggesting a lodged component within LFA4 (Fig. 6). Mean lineation azimuths from clast macrofabrics within the red diamicton are highly variable and none match the direction of ice flow inferred from the orientation of the MSGLs (299°). Hence, there appears to be no systematic relationship between the fabric orientation within the red diamicton that comprises the MSGLs and former ice flow direction.

Collectively, therefore, we interpret the facies variations within LFA4 between stratified and massive diamictons as consistent with an origin for the red diamicton as a glacitectonite and, in the case of the massive facies, a hybrid subglacial till, formed by a combination of sediment deformation and lodgement with the variability reflecting differences in the degree of mixing and cumulative strain (cf. Hicock and Fuller, 1995; Nelson et al., 2005; Evans et al., 2006; Ó Cofaigh et al., 2011). In the case of MSGL01, stratigraphic logs from the red diamicton show that the lower 1–1.5 m are typically stratified but grade upwards into a more massive red diamicton. Such vertical transitions from stratified diamicton to massive diamicton are consistent with increasing vertical strain, sediment homogenisation and an increasingly mature till up-sequence (Boulton and Hindmarsh, 1987; Croot and Sims, 1996; Boulton et al., 2001).

Sandy lenses and horizons found within subglacial tills have also been interpreted as a product of transient episodes of ice-bed decoupling due to fluctuations in porewater pressure (cf. Piotrowski and Tulacyzk, 1999; Larsen et al., 2004; Piotrowski et al., 2006). The sandy horizons record periods of high porewater pressure resulting in ice-bed separation and meltwater deposition. With a subsequent fall in porewater pressure, ice-bed recoupling takes place and diamicton is deposited between the sandy horizons. In the case of LFA4, while it is possible that some of the sandy horizons could have formed in this way, we postulate that the majority are a product of erosion, rafting and attenuation into the base of the diamicton. This is suggested by the fact that attenuated

lenses and rafts can be traced downwards from the diamicton into the underlying outwash, and also by the fact that, in many places, the lenses often do not have very distinct contacts with the surrounding diamicton but, rather, are 'blurred' and appear to represent incomplete mixing (e.g., Fig. 8g). This appears to contrast with observations of sliding bed facies which have been shown to be laterally continuous for up to several metres, quite fine grained and typically flat-lying (Larsen et al., 2004; Piotrowski et al., 2006).

3.3.5. LFA 5 (gravel, sand, mud association)

LFA5 overlies the red subglacial diamicton of LFA4 and formed during deglaciation. Facies sequences of ripple-drift, cross-lamination with dropstones, poorly sorted gravelly outwash with contorted laminated sand pods, clasts clusters, outsized clasts in a sandy matrix, and rhythmically laminated silty sands with dropstones are consistent with glacilacustrine sedimentation (Shaw, 1975; Ashley, 2002). Rippled sands and gravelly outwash record ice-proximal glacilacustrine sedimentation by traction current activity and gravelly mass flows. The gravelly units are poorly-sorted, crudely bedded and texturally heterogeneous, ranging from clast- to matrix-supported and the presence of contorted interbeds of laminated sand within the gravelly units suggests the slumping and partial mixing of the sands with the gravelly mass flows during downslope resedimentation. The presence of intact, albeit contorted, interbeds of sand associated with the gravels suggest that transport distances were short (Eyles and Eyles, 2000). Dropstones within the finer-grained sand and laminated mud indicates sediment delivery by iceberg rafting and, therefore, the presence of a lake(s) that was sufficiently deep to allow iceberg calving and rafting. LFA5 comprises an overall fining upwards sequence from gravely mass flows to laminated silty sand with dropstones which is interpreted to record an increasingly ice-distal depositional environment.

4. Discussion

4.1. Composition and internal structure of MSGLs and comparison to other studies

Stokes and Clark (2004) proposed that the Dubawnt Lake Palaeo-Ice Stream was triggered by the development of a proglacial lake during deglaciation which induced high calving rates and ice drawdown. While the trigger for the onset of streaming may have been the formation of a proglacial lake, our observations from sections along the Finnie River show that MSGL formation was intimately related to the presence of a thick glacifluvial deglacial sediment pile(s) which was overridden during streaming flow. This is also supported by the fact that observations from areas between MSGLs indicate that sediment cover is relatively thin and bedrock is observed within 2 m of the surface in our study area (Fig. 10). We suggest, therefore, that a pre-condition for MSGL formation is the presence of abundant sediments which are available for subglacial reworking during streaming. Exposures along the Finnie River show that MSGLs of the Dubawnt Lake Palaeo-Ice Stream are characterised by a red sandy diamicton that ranges from stratified to massive in structure and contains deformed interbeds and inclusions of sandy and gravelly outwash. The red diamicton overlies a thick sequence of glacifluvial outwash and formation of the diamicton is related to the subglacial overriding and reworking of this outwash when the ice stream was active. The resulting sediment is a glacitectonite that, in places, is transitional to a hybrid till. Stratification within the diamicton is a product of subglacial cannibalization and deformation of the underlying pre-existing outwash of LFA3. The degree of deformation and mixing of outwash within the diamicton is inferred to reflect variations in transport distance and cumulative strain. The well preserved nature of many of these inclusions throughout the red diamicton in MSGL03 and MSGL04 (Fig. 5) implies that deformation was not pervasive and, instead, that transport distances were relatively short ($\leq$1–2 km), the material subjected to low cumulative strain, and the depth of deformation relatively shallow. The sedimentological and clast macrofabric data are consistent with a combination of both non-pervasive deformation and lodgement occurring during formation of the red diamicton. In MSGL01, the lower parts of the red diamicton contain well preserved interbeds and lenses of sand derived from LFA3, and the diamicton is transitional from massive to locally stratified. This is also consistent with non-pervasive deformation and short transport distances. However, at this site, lithofacies logs show that the red diamicton becomes more massive vertically upsequence (Fig. 4). The latter observation is compatible with increasing cumulative strain and homogenization, and is perhaps also suggestive of the upper part of the red diamicton at MSGL01 containing a more mature, far-travelled component.

Fig. 10. Photograph of *in situ* sandstone bedrock overlain by 2 m of poorly exposed sandy diamicton (interpreted as till) from inter-ridge area of MSGLs along Finnie River. This contrasts with sediment thicknesses of over 10 m within the MSGL ridges themselves (see Figs. 3–5).

Our observations are similar to those reported by Shaw et al. (2000) in their study of the internal structure of an MSGL ridge in the Athabasca fluting field, Alberta. These authors described variably deformed, but usually well preserved, sandy sediment lenses and rafts within the lineation. Although Shaw et al. interpret the lineation as the product of erosion by a catastrophic subglacial meltwater flood, the preservation and abundance of the sandy inclusions within the Athabasca flutings could alternatively reflect short transport distances, non-pervasive deformation and low cumulative strain. Our observations are also consistent with work by Lemke (1958) and Evans (1996) who emphasized the importance of pre-exiting sediment depocentres that were overridden and reworked subglacially into MSGLs. In the case of the Dubawnt Lake MSGLs, the coarse-grained glacifluvial outwash of LFA3 acted as a source of the MSGL till and formed stable cores which were reworked into the lineations.

Some of the most detailed work on the sedimentology and internal composition of MGSLs has been carried out on the Antarctic continental shelf, where MSGLs that formed during ice stream flow across the shelf have been investigated using sediment cores and geophysical techniques (e.g., Wellner et al., 2001; Lowe and Anderson, 2002; Shipp et al., 2002; Graham et al., 2009). There, a number of studies have shown that MSGLs are formed

predominantly in a soft, porous, subglacial till with typical shear strengths of 0–20 kPa and average porosities of 40–50% (Dowdeswell et al., 2004; Ó Cofaigh et al., 2005, 2007; Evans et al., 2005; Reinardy et al., 2011; Livingstone et al., 2012). This soft till is generally accepted as having been formed during streaming flow by the subglacial reworking of pre-existing sediments on the shelf which ranged from glacimarine deposits to a stiff subglacial till deposited across the shelf prior to the onset of streaming flow. Although the soft till was initially suggested to have formed by subglacial deformation and the underlying stiff till by lodgement (e.g., Wellner et al., 2001), subsequent work indicates that they are both hybrid tills and formed by a combination of these processes (Ó Cofaigh et al., 2007).

A common finding that emerges therefore from our study and previous work is that MSGLs are frequently a product of the overriding and deformation of pre-existing sediments. Hence, the presence of a supply of pre-existing sediment which is then reworked subglacially during streaming flow appears to be an important control on MSGL formation. This idea is also consistent with the notion that many ice streams that operate across relatively flat beds require a pre-existing sedimentary bed to help lubricate flow (Bell et al., 1998). The alternative interpretation is that the MSGL ridges are a product of subglacial erosion and entrainment of sediment up-flow with subsequent subglacial transport into the area and deposition of this sediment to form the ridges. However, this is not supported by the sedimentology of the red till, which indicates reworking of pre-existing glacifluvial outwash and often short-transport distances. Such short transport distances and non-pervasive sediment deformation may, at least in part, reflect the short-lived duration of the Dubawnt Lake Palaeo-Ice Stream which has been suggested to have operated for only a few hundred years just prior to 8.2 ^{14}C ka BP and close to final deglaciation (Stokes and Clark, 2003). These observations are also consistent with the notion that ice stream motion was accommodated by shallow subglacial sediment deformation, perhaps accompanied transiently by basal sliding, rather than pervasive deformation of the ice stream bed.

4.2. Implications for formational theories of MSGLs

An important observation is that the MSGLs along the Finnie River contain both till and pre-existing glacifluvial sediments preserved within some ridges. This indicates that subglacial sediment deformation contributed to the genesis of these bedforms, but our results suggest that till deformation was commonly non-pervasive and associated sediment transport distances were relatively short. This is an interesting finding given that MSGLs along the Finnie River are sometimes in excess of 10 km long. Indeed, it suggests that these sedimentary bedforms are unlikely to be a product of a single point source initiation and downflow attenuation by pervasive subglacial sediment deformation (cf. Boulton and Hindmarsh, 1987; Boulton and Hindmarsh, 1987; Clark, 1993), but rather that sediment is eroded and incorporated into an MSGL ridge from a pre-existing substrate along the length of the landform. The coincidence of both erosion from between ridges and deposition/deformation along them is also consistent with the morphometry of the landforms, which suggests that the very longest MSGLs are also the narrowest (see Paper 1, Stokes et al., 2013), i.e. their great length develops more quickly than, or perhaps at the expense of, their width. Thus, in regions of thin till cover, it is conceivable that focused erosion in the inter-ridge 'grooves' could reach the underlying bedrock, leaving MSGL ridges perched on a bedrock surface, as observed on Coats and Southampton Islands, northern Canada (Ross et al., 2011).

Formation of the red diamicton and MSGL ridges by subglacial reworking and deformation of a pre-existing substrate is at least partially compatible with formation by some form of transient groove-ploughing (Clark et al., 2003). Ploughing of a soft sedimentary substrate would result in the deformation of that substrate and lateral accretion of sediment to form MSGL ridges (Tulaczyk et al., 2001; Clark et al., 2003). Indeed, evidence supporting such a process has been observed in marine geophysical records from palaeo-ice stream troughs in Antarctica (Ó Cofaigh et al., 2007). Thus, deformation of LFA3 and the presence of numerous contorted lenses and rafts of outwash within the red diamicton of LFA4 might reflect ploughing of the underlying outwash. Extending this explanation further, one might therefore expect to see lateral variations in stratigraphy and sediment deformation across an individual ridge, with perhaps truncation of pre-existing strata on either side (cf. Clark et al., 2003) and a decrease in deformation towards the ridge centre. However, our sedimentological observations from MSGLs along the Finnie River do not suggest lateral variations in strain and stratigraphy across the MSGL ridges, although the contrast between the MSGL orientation and the principal eigenvectors of the a-axis clast macrofabrics from the red 'MSGL till' mentioned above could reflect disturbance and lateral advection of pre-existing sediment during construction of the ridges through the groove-ploughing process.

Stokes et al. (2008) also reported sedimentological and geophysical data on the Dubawnt Lake Palaeo-Ice Stream bed at a location ~100 km northeast of the Finnie River, closer to the ice stream onset zone and attributed the presence of macrofabrics that trend transverse to the ice flow direction (inferred from the orientation of lineations) to compressive flow that coincided with ice stream shutdown. This interpretation was supported by: (i) the character and orientation of glaciotectonic structures in the MSGL sediment (till) indicative of brittle deformation, (ii) the flow direction inferred from the youngest striae on a boulder pavement in the till, and (iii) the presence and orientation of ribbed moraine that had formed on the MSGL ridges as a result of subglacial thrusting. However, since there is no geomorphological, sedimentological, or structural evidence of compressive flow at the Finnie River sites (the evidence instead points to mainly ductile deformation and extensional flow) it is likely that the transverse macrofabric observed there is a result of lateral flow of till into the ridges during their construction, as was predicted by Clark et al. (2003). Indeed, it is possible that the transverse fabrics observed at the Beverly Lake site are also a consequence of sediment advection during the formation of the MSGLs, rather than as a result of later compressive flow during ice stream shut down as originally proposed in Stokes et al. (2008).

An alternative explanation for removing/eroding material from between MSGL ridges to accentuate their length might be meltwater erosion. Indeed, Fowler (2010) has recently shown that the flow of a thin water film over soft sediments is unstable and rilling will occur, such that a series of flow-parallel streams develop, separated by intervening ridges (MSGLs). Fowler's (2010) mathematical treatment predicts a lateral spacing of a few hundred metres, with ridge amplitudes of the order of 10 m or so, which is consistent with observations made on the Dubawnt Lake Palaeo-Ice Stream bed (see Paper 1, Stokes et al., 2013). The precise nature of any resulting deposits is not specified but we did not observe any obvious meltwater-related deposits on-lapping the red till or on the flanks of the MSGLs. Note, however, that we were unable to observe exposures in the deepest part of the inter-ridge grooves. It is clear from our study, however, and indeed from the Antarctic shelf examples noted above, that MSGLs are unlikely to be a product of larger-scale, turbulent meltwater floods carving the lineations from a pre-existing substrate, but with little effect on the MSGL internal composition (cf. Shaw et al., 2000, 2008). This is because the tills within the MSGLs originate from the subglacial reworking of the

underlying outwash and they are deformed over 1–3 m thickness, although not pervasively. This is important sedimentological evidence, independent of other arguments against a meltwater origin discussed elsewhere (see King et al., 2009; Ó Cofaigh et al., 2010b; Paper 1,; Stokes et al., 2013). Therefore, whatever the formative mechanism, it appears to have modified the underlying sediments and reworked them subglacially into glacitectonites and hybrid tills. The alternative is that the red diamicton formed prior to MSGL formation, and that the lineations were subsequently carved into the deformed substrate represented by the red diamicton. Whilst we cannot completely rule out this alternative explanation, we suggest that it is less plausible because it both separates out the sedimentology of the bedforms from the process(es) of their formation and, perhaps more fundamental and problematic, it requires that their formation does not leave a recognisable sedimentological imprint in the stratigraphy.

5. Conclusions

- MSGLs are a characteristic subglacial landform formed during the interaction of streaming ice with a sedimentary bed. They have been documented from both modern and past ice sheets and, although their qualitative geomorphology and palaeoglaciological significance are known, the precise mechanism(s) responsible for their formation remains elusive. Existing theories range from long drumlins (Clark, 1993), to meltwater erosion (Shaw et al., 2008; Fowler, 2010), to spiral flows in glacial ice (Schoof and Clarke, 2008), to ploughing of the substrate by irregularly shaped ice keels (Clark et al., 2003). At least in part, this diversity of proposed mechanisms for their formation reflects the fact that there have actually been very few quantitative observations made of their morphology (cf. Stokes et al., 2013) and of their internal structure.
- Sediment exposures along the course of the Finnie River, which cuts across the former ice stream flow path, provide a window into the stratigraphy and sedimentology of MSGLs formed by the Dubawnt Lake Palaeo-Ice Stream. Formation of the MSGLs occurred during regional deglaciation (Stokes and Clark, 2003) and the overall stratigraphy shows that ice stream flow was preceded by an initial ice sheet advance from the southwest of either LGM or pre-LGM age, followed by ice sheet withdrawal and deposition of glacifluvial sediments. This was succeeded by the onset of streaming flow and MSGL formation. The final depositional event was the development of glacial lake(s) and glacilacustrine sedimentation following ice stream withdrawal.
- MSGLs along the Finnie River are dominated by a red diamicton lithofacies association, which comprises a stratified and massive (in places laminated), matrix-supported diamicton facies. Stratification is related to the reworking of underlying outwash over which the ice stream traversed, resulting in the presence of numerous interbeds, stringers and rafts of sorted sand and, in places, gravel, that are often contorted within the red diamicton.
- Sedimentological investigation of the red diamicton facies association (the 'MSGL till') shows that it is a hybrid till/glacitectonite formed by a combination of subglacial sediment deformation and lodgement. The source of the sediment for the red diamicton was the underlying glacifluvial outwash of LFA3 which was cannibalised during overriding by the ice stream and reworked subglacially, with the degree of deformation and mixing of this outwash into the red diamicton being a product of transport distance and cumulative strain. The often well preserved nature of many of the interbeds and rafts within the diamicton implies relatively short transport distances.
- Our results demonstrate the importance of sediment supply to MSGL formation in providing the material necessary for ridge formation. The Dubawnt Lake Palaeo-Ice Stream MSGLs are at least partially erosional (cf. Paper 1, Stokes et al., 2013) and relate to the overriding and reworking of pre-existing sediments. When compared with existing theories of MSGL formation, our sedimentological observations from the Dubawnt Lake Palaeo-Ice Stream bed are difficult to reconcile with the catastrophic meltwater hypothesis (Shaw et al., 2008), but are broadly consistent with formational theories that invoke at least partial erosion and reworking of material from between ridges, e.g. groove-ploughing of ice keels (Clark et al., 2003) and/or subglacial streams directed along inter-ridge grooves (Fowler, 2010). The key implication is that production of MSGLs appears to involve a combination of both sediment deformation and erosional processes which also explains why ice streams have the potential for rapid erosion over short timescales (e.g. Smith et al., 2012).

Acknowledgements

This research was funded by UK NERC grants NER/M/S/2003/00050 to Chris Stokes and NE/B501171/1 to Colm Ó Cofaigh. Olav Lian was funded in part by a Natural Science and Engineering Research Council (NSERC) of Canada Discovery Grant. Thanks to Rob Currie and Mark Loewen for excellent field and logistical support. We thank Martin Ross and the two anonymous reviewers whose comments led to improvements in the manuscript.

References

Ashley, G.M., 2002. Glaciolacustrine environments. In: Menzies, J. (Ed.), Modern and Past Glacial Environments. Butterworth-Heinemann, Oxford, pp. 417–444.
Aylsworth, J.M., Shilts, W.W., 1989. Bedforms of the Keewatin ice sheet, Canada. Sedimentary Geology 62, 407–428.
Banham, P.H., 1977. Glacitectonites in till stratigraphy. Boreas 6, 101–105.
Bell, R.E., Blankenship, D.D., Finn, C.A., Morse, D.L., Scambos, T.A., Brozena, J.M., Hodge, S.M., 1998. Influence of subglacial geology on the onset of a West Antarctic ice stream from aerogeophysical observations. Nature 394 (6688), 58–62.
Benn, D.I., 1994. Fabric shape and the interpretation of sedimentary fabric data. Journal of Sedimentary Research A64, 910–915.
Benn, D.I., Evans, D.J.A., 1996. The interpretation and classification of subglacially-deformed materials. Quaternary Science Reviews 15, 23–52.
Benn, D.I., 1995. Fabric signature of till deformation, Breiðamerkurjökull, Iceland. Sedimentology 42, 735–747.
Boothroyd, J.C., Ashley, G.M., 1975. Processes, bar morphology, and sedimentary structures on braided outwash fans, northeastern Gulf of Alaska. In: Jopling, A.V., McDonald, B.C. (Eds.), Glaciofluvial and Glaciolacustrine Sedimentation, SEPM Special Publication, vol. 23, pp. 193–222.
Boulton, G.S., Paul, M.A., 1976. The influence of genetic processes on some geotechnical properties of glacial tills. Quarterly Journal of Geological Engineering 9, 159–194.
Boulton, G.S., Hindmarsh, R.C.A., 1987. Sediment deformation beneath glaciers: rheology and sedimentological consequences. Journal of Geophysical Research 92 (B9), 9059–9082.
Boulton, G.S., Dobbie, K.E., Zatsepin, S., 2001. Sediment deformation beneath glaciers and its coupling to the subglacial hydraulic system. Quaternary International 86, 3–28.
Boyce, J.I., Eyles, N., 2000. Architectural element analysis applied to glacial deposits: internal geometry of a late Pleistocene till sheet, Ontario, Canada. Bulletin of the Geological Society of America 112, 98–118.
Clark, C.D., 1993. Mega-scale glacial lineations and cross-cutting ice-flow landforms. Earth Surface Processes and Landforms 18, 1–29.
Clark, C.D., Stokes, C.R., 2001. Extent and basal characteristics of the M'Clintock Channel Ice Stream. Quaternary International 86, 81–101.
Clark, C.D., Tulaczyk, S.M., Stokes, C.R., Canals, M., 2003. A groove-ploughing theory for the production of mega-scale glacial lineations, and implications for ice-stream mechanics. Journal of Glaciology 49, 240–256.
Clark, P.U., 1991. Striated clast pavements: products of deforming subglacial sediment? Geology 19, 530–533.
Croot, D.G., Sims, P.C., 1996. Early stages of till genesis: an example from Fanore, County Clare, Ireland. Boreas 25, 37–46.
Davies, B.J., Roberts, D.H., Ó Cofaigh, C., Bridgland, D.R., Riding, J.B., Teasdale, D.A., 2009. Interlobate ice sheet dynamics during the Last Glacial Maximum at Whitburn Bay, County Durham, England. Boreas 38, 555–578.

Dowdeswell, J.A., Ó Cofaigh, C., Pudsey, C.J., 2004. Thickness and extent of the subglacial till layer beneath an Antarctic paleo-ice stream. Geology 32, 13–16.
Dreimanis, A., 1992. Downward injected till wedges and upward injected till dikes. Sveriges Geologiska Undersökning 81, 91–96.
Dyke, A.S., Prest, V.K., 1987. Late Wisconsinan and Holocene history of the Laurentide ice sheet. Géographie Physique et Quaternaire 41, 237–263.
Evans, D.J.A., 1996. A possible origin for a megafluting complex on the southern Alberta prairies, Canada. Zeitschrift für Geomorphologie 106 (Suppl. Bd), 125–148.
Evans, D.J.A., Hiemstra, J.F., 2005. Till deposition by glacier submarginal, incremental thickening. Earth Surface Processes and Landforms 30, 1633–1662.
Evans, D.J.A., Phillips, E.R., Hiemstra, J.F., Auton, C.A., 2006. Subglacial till: formation sedimentary characteristics and classification. Earth Science Reviews 78, 115–176.
Evans, D.J.A., Hiemstra, J.F., Ó Cofaigh, C., 2007. An assessment of clast macrofabrics in glacigenic sediments based on A/B plane data. Geografiska Annaler 89, 103–120.
Evans, J., Pudsey, C.J., Ó Cofaigh, C., Morris, P.W., Domack, E.W., 2005. Late Quaternary glacial history, dynamics and sedimentation of the eastern margin of the Antarctic Peninsula Ice Sheet. Quaternary Science Reviews 24, 741–774.
Eyles, C.H., Eyles, N., 2000. Subaqueous mass-flow origin for Lower Permian diamictites and associated facies of the Grant Group, Barbwire terrace, Canning Basin, Western Australia. Sedimentology 47, 343–356.
Fowler, A.C., 2010. The formation of subglacial streams and mega-scale glacial lineations. Proceedings of the Royal Society of London, Series A 466 (2123), 3181–3201.
Graham, A.G.C., Later, R.D., Gohl, K., Hillenbrand, C.-D., Smith, J.A., Kuhn, G., 2009. Bedform signature of a West Antarctic ice stream reveals a multi-temporal record of flow and substrate control. Quaternary Science Reviews 28, 2774–2793.
Heroy, D., Anderson, J.B., 2005. Ice-sheet extent of the Antarctic Peninsula region during the Last Glacial Maximum (LGM) – insights from glacial geomorphology. Geological Society of America Bulletin 117, 1497–1512.
Hicock, S.R., 1991. On subglacial stone pavements in till. Journal of Geology 99, 607–619.
Hicock, S.R., Fuller, E.A., 1995. Lobal interactions, rheologic superimposition, and implications for a Pleistocene ice stream on the continental shelf of British Columbia. Geomorphology 14, 167–184.
Hicock, S.R., Goff, J.R., Lian, O.B., Little, E.C., 1996. On the interpretation of subglacial till fabric. Journal of Sedimentary Research 66, 928–934.
Hiemstra, J., Evans, D.J.A., Ó Cofaigh, C., 2007. The role of glaciotectonic rafting and comminution in the production of subglacial tills: examples from SW Ireland and Antarctica. Boreas 36, 386–399.
Jørgensen, F., Piotrowski, J.A., 2003. Signature of the Baltic ice stream on Funen Island, Denmark during the Weichselian glaciation. Boreas 32, 242–255.
King, E.C., Hindmarsh, R.C.A., Stokes, C.R., 2009. Formation of mega-scale glacial lineations observed beneath a West Antarctic ice stream. Nature Geoscience v. 2, 585–596.
Kleman, J., Borgström, I., 1996. Reconstruction of palaeo-ice sheets: the use of geomorphological data. Earth Surface Processes and Landforms 21, 893–909.
Kleman, J., Jansson, K., De Angelis, H., Stroeven, A.P., Hattestrand, C., Alm, G., Glasser, N.F., 2010. North American Ice Sheet build-up during the last glacial cycle, 115-21 kyr. Quaternary Science Reviews 29, 17–18.
Larsen, N.K., Piotrowski, J.A., Kronborg, C., 2004. A multiproxy study of a basal till: a time- transgressive accretion and deformation hypothesis. Journal of Quaternary Science 19, 9–21.
Lemke, R.W., 1958. Narrow linear drumlins near Velva, north Dakota. American Journal of Science 256, 270–283.
Lian, O.B., Hicock, S.R., 2000. Thermal conditions beneath parts of the last Cordilleran Ice Sheet near its centre as inferred from subglacial till, associated sediments and bedrock. Quaternary International 68–71, 147–162.
Lian, O.B., Hicock, S.R., 2010. Insight into the character of palaeo-ice flow in upland regions of mountain valleys during the last major advance (Vashon Stade) of the Cordilleran Ice Sheet, southwest British Columbia. Boreas 39, 171–186.
Livingstone, S.J., Ó Cofaigh, C.O., Stokes, C.R., Hillenbrand, C.-D., Vieli, A., Jamieson, S.R., 2012. Antarctic palaeo-ice streams. Earth-Science Reviews 111, 90–128.
Lowe, A.L., Anderson, J.B., 2002. Reconstruction of the West Antarctic ice sheet in Pine Island Bay during the Last Glacial Maximum and its subsequent retreat history. Quaternary Science Reviews 21, 1879–1897.
McMartin, I., Henderson, P.J., 2004. Evidence from Keewatin (Central Nunavut) for paleo-ice divide migration. Géographie physique et Quaternaire 58, 163–186.
McMartin, I., Dredge, L.A., Ford, K.L., Kjarsgaard, I.M., 2006. Till Composition, Provenance and Stratigraphy Beneath the Keewatin Ice Divide, Schultz Lake Area (NTS 66A), Mainland Nunavut. In: Geological Survey of Canada, p. 81. Open File 5312.
Miall, A.D., 1992. Alluvial deposits. In: Walker, R.G., James, N.P. (Eds.), Facies Models: Response to Sea-level Change. Geological Association of Canada, Toronto, pp. 119–142.
Nelson, A.E., Willis, I.C., Ó Cofaigh, C., 2005. Till genesis and glacier motion inferred from sedimentological evidence associated with the surge-type glacier, Bruarjokull, Iceland. Annals of Glaciology 42, 14–22.
Ó Cofaigh, C., Pudsey, C.J., Dowdeswell, J.A., Morris, P., 2002. Evolution of subglacial bedforms along a paleo-ice stream, Antarctic Peninsula continental shelf. Geophysical Research Letters 29 (8). http://dx.doi.org/10.1029/2001GL014488.
Ó Cofaigh, C., Dowdeswell, J.D., Allen, C.S., Hiemstra, J.F., Pudsey, C.F., Evans, J., Evans, D.J.A., 2005. Flow dynamics and till genesis associated with a marine-based Antarctic palaeo-ice stream. Quaternary Science Reviews 24, 709–740.
Ó Cofaigh, C., Evans, J., Dowdeswell, J.A., Larter, R.D., 2007. Till characteristics, genesis and transport beneath Antarctic paleo-ice streams. Journal of Geophysical Research 112, F03006. http://dx.doi.org/101029/2006JF000606.
Ó Cofaigh, C., Evans, D.J.A., Smith, I.R., 2010a. Large-scale reorganization and sedimentation of terrestrial ice streams during late Wisconsinan Laurentide Ice Sheet deglaciation. Geological Society of America Bulletin 122, 743–756.
Ó Cofaigh, C., Dowdeswell, J.A., King, E., Anderson, J.B., Clark, C.D., Evans, D.J.A., Evans, J., Hindmarsh, R.C.A., Larter, R.D., Stokes, C.R., 2010b. Comment on Shaw J., Pugin, A. and Young, R. (2008): "A meltwater origin for Antarctic shelf bedforms with special attention to megalineations" Geomorphology 102, 364–375. Geomorphology 117, 195–198.
Ó Cofaigh, C., Evans, D.J.A., Hiemstra, J., 2011. Formation of a stratified subglacial "till" (glacitectonite) assemblage by ice-marginal thrusting and glacier overriding. Boreas 40, 1–14.
Ottesen, D., Dowdeswell, J.A., rise, L., 2005. Submarine landforms and the reconstruction of fast-flowing ice streams within a large Quaternary ice sheet: the 2500-km-long Norwegian- Svalbard margin (57°–80°N). Geological Society of America Bulletin 117, 1033–1050.
Piotrowski, J.A., Tulacyzk, S., 1999. Subglacial conditions under the last ice sheet in northwest Germany: ice-bed separation and enhanced basal sliding? Quaternary Science Reviews 18, 737–751.
Piotrowski, J.A., Larsen, N.K., Menzies, J., Wysota, W., 2006. Formation of subglacial till under transient bed conditions: deposition, deformation, and basal decoupling under a Weichselian ice sheet lobe, central Poland. Sedimentology 53, 83–106.
Reinardy, B.T.I., Hiemstra, J., Murray, T., Hillenbrand, C.-D., Larter, R., 2011. Till genesis at the bed of an Antarctic Peninsula palaeo-ice stream as indicated by micromorphological analysis. Boreas 40, 498–517.
Ross, M., Lajeunesse, P., Kosar, A., 2011. The subglacial record of northern Hudson Bay: insights into the Hudson Strait Ice Stream catchment. Boreas 40 (1), 73–91.
Schoof, C., Clarke, G.K.C., 2008. A model for spiral flows in basal ice and the formation of subglacial flutes based on a Reiner-Rivlin rheology for glacial ice. Journal of Geophysical Research 113, B05204.
Shaw, J., 1975. Sedimentary successions in Pleistocene ice-marginal lakes. In: Jopling, A.V., McDonald, B.C. (Eds.), Glaciofluvial and Glaciolacustrine Sedimentation, SEPM, Special Publication, vol. 23, pp. 281–303.
Shaw, J., Faragini, D.M., Kvill, D.R., Rains, B.R., 2000. The Athabasca fluting field, Alberta, Canada: implications for the formation of large-scale fluting (erosional lineations). Quaternary Science Reviews 19 (10), 959–980.
Shaw, J., Pugin, A., Young, R.R., 2008. A meltwater origin for Antarctic shelf bedforms with special attention to megalineations. Geomorphology 102, 364–375.
Shipp, S.S., Anderson, J.B., Domack, E.W., 1999. Late Pleistocene-Holocene retreat of the West Antarctic Ice-Sheet system in the Ross Sea: part 1 – geophysical results. Geological Society of America Bulletin 111, 1486–1516.
Shipp, S.S., Wellner, J.S., Anderson, J.B., 2002. Retreat signature of a polar ice stream: sub-glacial geomorphic features and sediments from the Ross Sea, Antarctica. In: Dowdeswell, J.A., Ó Cofaigh, C. (Eds.), Glacier-influenced Sedimentation on High-latitude Continental Margins, Geological Society, London, Special Publication, vol. 203, pp. 277–304.
Smith, A.M., Bentley, C.R., Bingham, R.G., Jordan, T.A., 2012. Rapid subglacial erosion beneath Pine Island Glacier, West Antarctica. Geophysical Research Letters 39, L12501. http://dx.doi.org/10.1029/201GL051651.
Stokes, C.R., Clark, C.D., 1999. Geomorphological criteria for identifying Pleistocene ice streams. Annals of Glaciology 28, 67–74.
Stokes, C.R., Clark, C.D., 2002. Are long subglacial bedforms indicative of fast ice flow? Boreas 31, 239–249.
Stokes, C.R., Clark, C.D., 2003. The Dubawnt Lake palaeo-ice stream: evidence for dynamic ice sheet behaviour on the Canadian Shield and insights regarding the controls on ice stream location and vigour. Boreas 32, 263–279.
Stokes, C.R., Clark, C.D., 2004. Evolution of late glacial ice-marginal lakes on the northwestern Canadian Shield and their influence on the location of the Dubawnt Lake palaeo-ice stream. Palaeogeography, Palaeoclimatology, Palaeoecology 215, 155–171.
Stokes, C.R., Lian, O.B., Tulaczyk, S., Clark, C.D., 2008. Superimposition of ribbed moraines on a palaeo-ice-stream bed: implications for ice stream dynamics and shutdown. Earth Surface Processes and Landforms 33, 593–609.
Stokes, C.R., Spagnolo, M., Clark, C.D., 2011. The composition and internal structure of drumlins: complexity, commonality, and implications for a unifying theory of their formation. Earth-Science Reviews 107, 398–422.
Stokes, C.R., Spagnolo, M., Clark, C.D., Tulaczyk, S.M., Ó Cofaigh, C., Lian, O., Dunstone, R.B., 2013. Formation of Mega-scale Glacial Lineations on the Dubawnt Lake Ice Stream bed: 1. Size, Shape and Spacing from a Large Remote Sensing Dataset. Quaternary Science Reviews 77, 190–209.
Tulaczyk, S.M., Scherer, R.P., Clark, C.D., 2001. A ploughing model for the origin of weak tills beneath ice streams: a qualitative treatment. Quaternary International 86 (1), 59–70.
Wellner, J.S., Lowe, A.L., Shipp, S.S., Anderson, J.B., 2001. Distribution of glacial geomorphic features on the Antarctic continental shelf and correlation with substrate: implications for ice behaviour. Journal of Glaciology 47, 397–411.